Multiquark Hadrons - Current Status and Issues

Ahmed Ali *

Deutsches Elektronen-Synchrotron DESY,
D-22607 Hamburg, Germany
*E-mail: ahmed.ali@desy.de

DOI: http://dx.doi.org/10.3204/DESY-PROC-2016-04/Ali

Multiquark states having four and five valence quarks, called tetraquarks and pentaquarks, respectively, are now firmly established experimentally, with the number of such independent states increasing steadily over the years. They represent a new facet of QCD, but the underlying dynamics is currently poorly understood. I review some selected aspects of data and discuss several competing phenomenological models put forward to accommodate them.

1 Introduction

Ever since the discovery of the state $X(3872)$ by Belle in 2003 [1], a large number of multiquark states has been discovered in particle physics experiments, conducted at the electron-positron and hadron colliders. They are exotic, having J^{PC} quantum numbers not allowed for $q\bar{q}$ states, or have too small a decay width for their mass, and, in some cases, their decay distributions have unfamiliar features not seen before. Most of them are quarkonium-like states, in that they have a $(c\bar{c})$ or a $(b\bar{b})$ component in their Fock space. A good fraction of them are electrically neutral but some are singly-charged. Examples are $X(3872)(J^{PC} = 1^{++})$, $Y(4260)(J^{PC} = 1^{--})$, $Z_c(3900)^{\pm}(J^P = 1^+)$, $P_c(4450)^{\pm}(J^P = 5/2^+)$, in the hidden charm sector, and $Z_b(10610)^{\pm}(J^P = 1^+)$ and $Z_b(10650)^{\pm}(J^P = 1^+)$, in the hidden bottom sector. The numbers in the parentheses are their masses in MeV. Of these, $P_c(4450)^{\pm}(J^P = 5/2^+)$ is a pentaquark state, as its discovery mode $P_c(4450)^+ \to J/\psi p$ [2] requires a minimal valence quark content $c\bar{c}uud$. The others are tetraquark states, with characteristic decays, such as $X(3872) \to J/\psi\pi^+\pi^-$, $Y(4260) \to J/\psi\pi^+\pi^-$, $Z_c(3900)^+ \to J/\psi\pi^+$, and $Z_b(10610)^+ \to h_b(1P, 2P)\pi^{\pm}, \Upsilon(1S, 2S)\pi^+$. The charmonia sector and the observed neutral charmonium-like exotic states are shown in Fig. 1, and the observed charged charmonium-like states are displayed in Fig. 2. No doubly-charged multiquark hadron has been seen so far, though some are expected, such as $[\bar{c}\bar{u}][sd] \to D_s^-\pi^-$, in the diquark scenario discussed below.

Deciphering the underlying dynamics of the multiquark states is a formidable challenge and several models have been proposed to accommodate them. I discuss them briefly in the next section for the tetraquark mesons, and will discuss one of them - the diquark model - in some details in section 3. Current data and models for the observed pentaquarks are discussed briefly in section 4, and the diquark model for pentaquarks is discussed at some length in section 5, including a number of predictions to be tested in forthcoming experiments. A summary is given

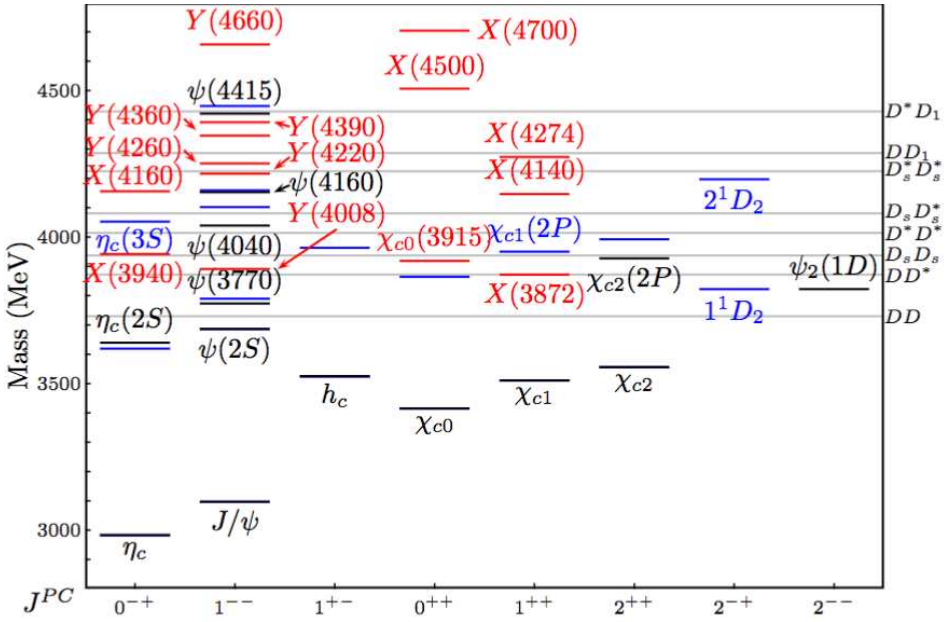

Figure 1: Charmonia and Charmonium-like neutral exotic sector. Black lines represent observed charmonium levels, blue lines are predicted charmonia levels and red lines are exotic states. Two-particle meson thresholds are indicated on the right (from [3]).

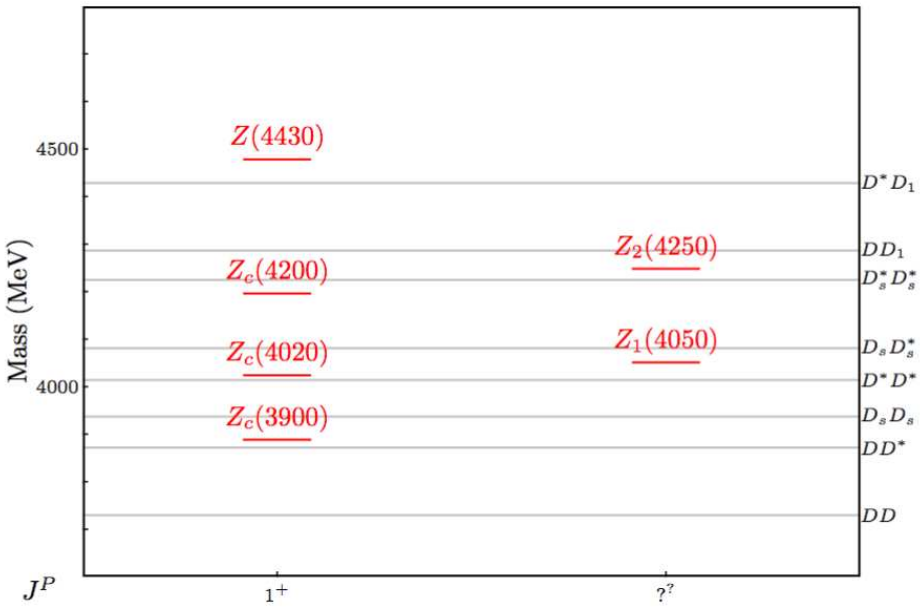

Figure 2: Observed charged exotic charmonium sector. Two-particle meson thresholds are indicated on the right (from [3]).

in section 6.

2 Models for Tetraquarks

Several explicit kinematic and dynamical mechanisms have been devised to accommodate the exotic spectroscopy. They go by the names: cusps, hadroquarkonia, hybrids, hadron molecules, and compact diquarks. They are briefly explained below.

2.1 Tetraquarks as Cusps

In the cusp interpretation of tetraquarks [4, 5], it is assumed that threshold re-scatterings are enough to describe the data, and as such there is no need for poles in the scattering matrix. This approach has been invoked to explain the origin of the charged states $Z_c(3900)[D\bar{D}^*]$, $Z_c(4025)[D^*\bar{D}^*]$, $Z_b(1610)[B\bar{B}^*]$, and $Z_b(10650)[B^*\bar{B}^*]$, as they lie just above the indicated thresholds. Discussed long ago by Wigner [6] in the context of the non-relativistic two-body scattering theory, and stressed more recently by Törnqvist [7] in an attempt to understand the low-lying scalar meson $q\bar{q}$ nonet, and by Bugg [8], in interpreting the resonances as synchronized artefacts, this effect has to do with the behavior of scattering cross-sections $\sigma(E)$ near thresholds, say $E = E_0$. The cross-section remains finite as one approaches E_0 from above or below, but the slope $d\sigma(E)/dE$ shows a discontinuity, which can result in a "cusp", as $\sigma(E)$ is continued below E_0. It is related to the self-energy threshold singularity, in that the expression for the imaginary part of the self-energy $\mathrm{Im}\Pi(s)$ is zero for $\sqrt{s}$ below the threshold and turns on rapidly once the threshold is crossed[1]. Here $\Pi(s)$ is the self-energy of of a particle coupled to two intermediate states. The resulting enhancements by cusps can mimic genuine S-matrix poles (resonances). However, they can be distinguished by studying the phase motions of the amplitudes. Representing a resonance by a Breit-Wigner amplitude, $f(s) = \Gamma/2/(M - \sqrt{s} - i\Gamma/2)$, the magnitude and phase vary with $\sqrt{s}$, according to a circular trajectory in the Argand diagram. Cusps, on the other hand, have characteristically different dependence on $\sqrt{s}$. Using the variable $z = c(m_A + m_B - \sqrt{s})$, where A and B are the intermediate states, and c is a normalizing constant, one can show that the imaginary part of a cusp amplitude is zero for positive z (i.e., below threshold) and turns on rapidly as the threshold is crossed, reflecting essentially the function $erfc(\sqrt{z})$, which governs $\mathrm{Im}(\Pi(s))$. This phase motion differs from that of a genuine Breit-Wigner. We will illustrate this in the context of the pentaquark $P_c(4450)^+$ later in section 4.

2.2 Tetraquarks as hadroquarkonia

This mechanism is motivated by analogy with the hydrogen atom. In the hadroquarkonium model, a $Q\bar{Q}$ ($Q = c, b$) forms the hard core surrounded by light matter (light $q\bar{q}$ in the case of tetraquarks and qqq for pentaquarks), with the two systems bound by a van der Walls type force. For example, the hadrocharmonium core may consist of the $J/\psi, \psi'$ or χ_c, and the light $q\bar{q}$ degrees of freedom can be combined to accommodate the observed hadrons [9]. A variation on this theme is that the hard core quarkonium could be in a color-adjoint representation, in which case the light degrees of freedom are also a color-octet to form an overall singlet. Hadroquarkonium models have conceptual problems, in that if the binding force is weak, the

[1] Here E and $\sqrt{s}$ are used interchangeably.

question is why the system remains stable for long enough a time to be identified as a distinct state. If the force is strong, it is not clear why the $Q\bar{Q}$ core and the light degrees of freedom don't rearrange themselves as a pair of heavy mesons ($D\bar{D}^*, B\bar{B}^*$ etc.). This would then suppress the appearance of the states $(J/\psi, h_c)\pi\pi$ in their decays, which, in fact, are the discovery modes of many such exotic multiquark states.

2.3 Tetraquarks as hybrids

Next are hybrid models, the basic idea of which dates back to circa 1994 [10] based on the QCD-inspired flux-tubes, which predict exotic $J^{\rm PC}$ states of both the light and heavy quarks. Hybrids are hadrons formed from valence quarks and gluons, for example, consisting of $Q\bar{Q}g$. States dominated by gluons form glueballs, which are firm predictions of QCD, but have proven to be elusive experimentally. What has emerged from the current lattice-QCD computations [11] is that non-perturbative gluons, the object of interest in constructing the hybrids, are quasiparticles having $J^{PC} = 1^{+-}$ with an excitation energy of approximately 1 GeV. This would put the lightest charmonium multiplets at around 4200 MeV. Extensive studies of such hybrids have been carried out on the lattice by the Hadron Spectrum Collaboration [12], though for a heavy pion mass, $m_\pi \sim 400$ MeV and at fixed lattice spacing. Several states in this computation are identified as charmonium hybrid multiplets, having the quantum numbers $J^{PC} = 0^{-+}, 1^{--}, 2^{-+}, 1^{-+}$, with their masses ($M$) estimated to lie in the range $M - M_{\eta_c} \simeq 1200 - 1400$ MeV. Very much along the same lines, but much earlier, a hybrid interpretation was advanced for the $J^{\rm PC} = 1^{--}$ state $Y(4260)$, which has a small e^+e^- annihilation cross section [13, 14, 15]. In the meanwhile, hybrids have been offered as templates for other exotic hadrons as well [16, 17]. They have been put on firmer theoretical footings in the framework of effective field theories [18]. Despite all these theoretical advances, which are impressive and may eventually provide reliable quantitative predictions, an unambiguous hybrid candidate has yet to be identified in the current experiments. Advances in lattice QCD techniques, enabling a firm phenomenological profiles of the glueballs and the $Q\bar{Q}g$ hybrids, and dedicated experiments, such as the GlueX [19] and $\bar{\rm P}$ANDA [20], may change this picture dramatically.

2.4 Tetraquarks as hadron molecules

A very popular approach assumes that the tetraquark (pentaquark) states are meson-meson (meson-baryon) bound states, with an attractive residual van der Waals force generated by mesonic exchanges [21]. This hypothesis is in part supported by the closeness of the observed exotic hadron masses to their respective two-particle thresholds, as can be seen in Figs. 1 and 2. In many cases, this leads to a very small binding energy, which imparts the exotic hadrons very large hadronic radii, following from the Heisenberg uncertainty principle. This is best illustrated by the $X(3872)$, which has an S-wave coupling to $D^*\bar{D}$ (and its conjugate) and has a binding energy $\mathcal{E}_X = M_{X(3872)} - M_{D^{*0}} - M_{\bar{D}^0} = +0.01 \pm 0.18$ MeV. Such a hadron molecule will have a large mean square separation of the constituents $\langle r_X \rangle \propto 1/\sqrt{\mathcal{E}_X} \simeq 10$ fm, where the quoted radius corresponds to a binding energy $\mathcal{E}_X = 0.15$ MeV. This would lead to small production cross-sections in hadronic collisions [22], contrary to what has been observed in a number of experiments at the Tevatron and the LHC. In some theoretical constructs, this problem is mitigated by making the hadron molecules complicated by invoking a hard (point-like) core. In that sense, such models resemble hadroquarkonium models, discussed above. In

yet others, rescattering effects are invoked to substantially increase the cross-sections [23]. A crucial test is the p_T-spectrum of the exotic hadrons in question in prompt production processes at the LHC.

The hadron molecular picture is plausible in explaining some aspects of the current data, namely the lack of experimental evidence of a quartet of exotic states, almost degenerate in mass with the $X(3872)$, containing a light quark-antiquark pair $q\bar{q}$, $q = u, d$, leading to the formation of $I = 1$ and $I = 0$ multiplets. These multiplets are anticipated in the diquark picture, discussed below. However, in the molecular picture, due to the exchange of a pion providing the main binding, and pion being an isospin-1 meson, not all isospin configurations will bind. In line with this, no resonant structure is seen near the $D^0\bar{D}^0$ threshold, consistent with the inadmissibility of a strong interaction coupling of three pseudo-scalars $D^0\bar{D}^0\pi^0$ due to parity conservation. On the other hand, the case for hadron molecules is weak for those exotics whose masses are well above the respective thresholds. For example, the $Z_c(3900)^+$ is a case in point in which the mass lies 20 MeV above the $D\bar{D}^*$ threshold, which, incidentally, is also its main decay mode. This is hard to accommodate in the hadron molecular picture. Theoretical interest in hadron molecules has remained unabated, and there exists a vast and growing literature on this topic with ever increasing sophistication, a sampling of which is referenced here [24, 25, 26, 27, 28, 29, 30].

2.5 Tetraquarks as compact diquark-antidiquark mesons

Last, but by no means least, on this list are QCD-based interpretations in which tetraquarks and pentaquarks are genuinely new hadron species in which a color-nonsinglet diquark is the essential building block [31, 32, 33]. In the large N_c limit of QCD, tetraquarks, treated as diquark-antidiquark mesons, are shown to exist [34, 35, 36] as poles in the S-matrix. They may have narrow widths in this approximation, and hence they are reasonable candidates for multiquark states. First attempts to study multiquark states using Lattice QCD have been undertaken [37, 38, 39, 40, 41] in which correlations involving four-quark operators are studied numerically. Evidence of tetraquark states in the sense of S-matrix poles using these methods is still lacking. Establishing the signal of a resonance requires good control of the background. In the lattice QCD simulations of multiquark states, this is currently not the case. This may be traced back to the presence of a number of nearby hadronic thresholds and to lattice-specific issues, such as an unrealistic pion mass. More powerful analytic and computational techniques are needed to draw firm conclusions.

In the absence of reliable first principle calculations, approximate phenomenological methods are the way forward. In that spirit, an effective Hamiltonian approach has been often used [31, 32, 42, 43, 44, 45], in which tetraquarks are assumed to be diquark-antidiquark objects, bound by gluonic exchanges (pentaquarks are diquark-diquark-antiquark objects). This allows one to work out the spectroscopy and some aspects of tetraquark decays. Heavy quark symmetry is a help in that it can be used for the heavy-light diquarks relating the charmonia-like states to the bottomonium-like counterparts. As detailed below, diquark models anticipate a very rich spectroscopy of tetraquarks and pentaquarks, only a small part of which has been possibly observed experimentally. Hence, diquark models are in dire need of dynamical selection rules to reduce the number of observable states. The underlying dynamics is complex and the current theoretical framework, in which the parameters of the effective Hamiltonian subsume the dynamics, is obviously inadequate. I will discuss the phenomenology of the diquark picture in the next section to test how far such models go in describing the observed exotic hadrons

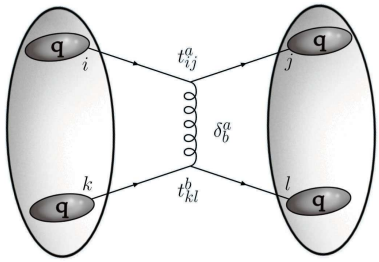

Figure 3: One-gluon exchange diagram for diquarks.

and other properties measured in current experiments.

For recent in-depth reviews of all the models discussed above and the theoretical techniques employed, see [3, 46, 47, 48].

3 The Diquark Model

The basic assumption of this model is that diquarks are tightly bound colored objects and they are the building blocks for forming tetraquark mesons and pentaquark baryons. Diquarks, for which we use the notation $[qq]_c$, and interchangeably $\mathcal{Q}$, have two possible SU(3)-color representations. Since quarks transform as a triplet $\mathsf{3}$ of color SU(3), the diquarks resulting from the direct product $\mathsf{3} \otimes \mathsf{3} = \bar{\mathsf{3}} \oplus \mathsf{6}$, are thus either a color anti-triplet $\bar{\mathsf{3}}$ or a color sextet $\mathsf{6}$. The leading diagram based on one-gluon exchange is shown in Fig. 3. The product of the SU(3)-matrices in Fig. 3 can be decomposed as

$$t^a_{ij} t^a_{kl} = -\frac{2}{3} \underbrace{(\delta_{ij}\delta_{kl} - \delta_{il}\delta_{kj})/2}_{\text{antisymmetric: projects } \bar{\mathbf{3}}} + \frac{1}{3} \underbrace{(\delta_{ij}\delta_{kl} + \delta_{il}\delta_{kj})/2}_{\text{symmetric: projects } \mathbf{6}} . \tag{1}$$

The coefficient of the antisymmetric $\bar{\mathsf{3}}$ representation is $-2/3$, reflecting that the two diquarks bind with a strength half as strong as between a quark and an antiquark, in which case the corresponding coefficient is $-4/3$. The symmetric $\mathsf{6}$ on the other hand has a positive coefficient, $+1/3$, reflecting a repulsion. Thus, in working out the phenomenology, a diquark is assumed to be an $SU(3)_c$-antitriplet, with the antidiquark a color-triplet. With this, we have two color-triplet fields, quark q_3 and anti-diquark $\overline{\mathcal{Q}}$ or $[\bar{q}\bar{q}]_3$, and two color-antitriplet fields, antiquark $\bar{q}_{\bar{3}}$ and diquark $\mathcal{Q}$ or $[qq]_{\bar{3}}$, from which the spectroscopy of the conventional and exotic hadrons is built. However, the quarks and diquarks differ in an essential point, namely the former are point-like objects but the latter are composite and have a hadronic size. It has crucial importance in determining the electromagnetic and strong couplings, and hence for the production cross-sections in leptonic and hadronic collisions.

Since quarks are spin-1/2 objects, a diquark has two possible spin-configurations, spin-0, with the two quarks in a diquark having their spin-vectors anti-parallel, and spin-1, in which case the two quark spins are aligned, as shown in Fig. 4. They were given the names "good diquarks" and "bad diquarks", respectively, by Jaffe [49], implying that in the former case, the two quarks bind, and in the latter, the binding is not as strong. There is some support of this pattern from lattice simulations for light diquarks [50], in which correlations are studied in

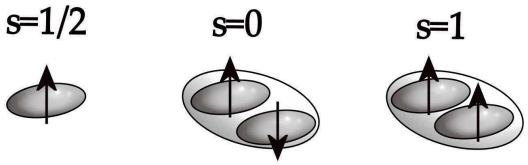

Figure 4: Quark and diquark spins.

terms of the spatial distribution of the two quarks forming the diquark in the background of the static quark. Phenomenological expectations that QCD dynamics favors the formation of good (spin-0) diquarks in color anti-triplet configuration is verified. It is exceedingly important to study on the lattice such correlations in two-point functions, involving tetraquarks, which have been attempted but with inconclusive results so far. However, as the spin-degree of freedom decouples in the heavy quark systems, as can be shown explicitly in heavy quark effective theory context for heavy mesons and baryons [51], we expect that this decoupling will also hold for heavy-light diquarks $[Q_i q_j]_{\bar{3}}$ with $Q_i = c, b; q_j = u, d, s$. So, for the heavy-light diquarks, both the spin-1 and spin-0 configurations are present. Also, the diquarks in heavy baryons (such as Λ_b and Ω_b), consisting of a heavy quark and a light diquark, both $j^p = 0^+$ and $j^p = 1^+$ quantum numbers of the diquark are needed to accommodate the observed baryon spectrum.

In this writeup, we will be mostly discussing heavy-light diquarks, though heavy-heavy diquarks $[QQ]_{\bar{3}}$ ($Q = c, b$), and the resulting tetraquark states $[QQ]_{\bar{3}}[\bar{Q}\bar{Q}]_3$ are also anticipated and discussed in the literature [52]. Following the discussion above, we construct the interpolating diquark operators for the two spin-states of such diquarks (here $Q = c, b$) [32]:

$$\begin{array}{rrrcl} \text{Scalar} & 0^+: & \mathcal{Q}_{i\alpha} & = & \epsilon_{\alpha\beta\gamma}(\bar{Q}_c^{\beta}\gamma_5 q_i^{\gamma} - \bar{q}_{i_c}^{\beta}\gamma_5 Q^{\gamma}), \qquad {\scriptstyle \alpha,\,\beta,\,\gamma:\ SU(3)_C \text{ indices}} \\ \text{Axial-Vector} & 1^+: & \vec{\mathcal{Q}}_{i\alpha} & = & \epsilon_{\alpha\beta\gamma}(\bar{Q}_c^{\beta}\vec{\gamma} q_i^{\gamma} + \bar{q}_{i_c}^{\beta}\vec{\gamma} Q^{\gamma}). \end{array}$$

In the non-relativistic (NR) limit, these states are parametrized by Pauli matrices: $\Gamma^0 = \frac{\sigma_2}{\sqrt{2}}$ (Scalar 0^+), and $\vec{\Gamma} = \frac{\sigma_2\vec{\sigma}}{\sqrt{2}}$ (Axial-Vector 1^+). We will characterize a tetraquark state with total angular momentum J by the state vector $|s_{\mathcal{Q}}, s_{\bar{\mathcal{Q}}};\ J\rangle$ showing the diquark spin $s_{\mathcal{Q}}$ and the antidiquark spin $s_{\bar{\mathcal{Q}}}$. There is no consensus on their names. We use the symbols X_J for J^{++}, Z for $J^{PC} = 1^{+-}$, and Y for $J^{PC} = 1^{--}$ states. Thus, the tetraquarks with the following diquark-spin and angular momentum J have the Pauli forms:

$$\begin{aligned} |0_{\mathcal{Q}}, 0_{\bar{\mathcal{Q}}};\ 0_J\rangle &= \Gamma^0 \otimes \Gamma^0, \\ |1_{\mathcal{Q}}, 1_{\bar{\mathcal{Q}}};\ 0_J\rangle &= \frac{1}{\sqrt{3}}\Gamma^i \otimes \Gamma_i, \\ |0_{\mathcal{Q}}, 1_{\bar{\mathcal{Q}}};\ 1_J\rangle &= \Gamma^0 \otimes \Gamma^i, \\ |1_{\mathcal{Q}}, 0_{\bar{\mathcal{Q}}};\ 1_J\rangle &= \Gamma^i \otimes \Gamma^0, \\ |1_{\mathcal{Q}}, 1_{\bar{\mathcal{Q}}};\ 1_J\rangle &= \frac{1}{\sqrt{2}}\varepsilon^{ijk}\Gamma_j \otimes \Gamma_k. \end{aligned} \tag{2}$$

Whenever necessary, we will put a subscript c or b to distinguish the $c\bar{c}$ and $b\bar{b}$ states.

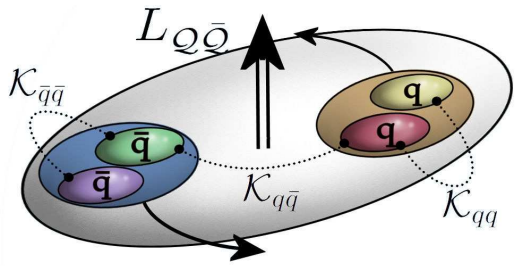

Figure 5: Schematic diagram of a tetraquark in the diquark-antidiquark picture.

3.1 Non-relativistic Hamiltonian for Tetraquarks with hidden charm

For the heavy quarkonium-like exotic hadrons, we work in the non-relativistic limit and use the following effective Hamiltonian to calculate the tetraquark mass spectrum [32, 42]

$$H_{\rm eff} = 2m_{\mathcal{Q}} + H_{SS}^{(qq)} + H_{SS}^{(q\bar{q})} + H_{SL} + H_{LL}, \tag{3}$$

where $m_{\mathcal{Q}}$ is the diquark mass, the second term above is the spin-spin interaction involving the quarks (or antiquarks) in a diquark (or anti-diquark), the third term depicts spin-spin interactions involving a quark and an antiquark in two different shells (i.e., in the two different diquark configurations), with the fourth and fifth terms being the spin-orbit and the orbit-orbit interactions, involving the quantum numbers of the tetraquark, respectively. For the S-states, these last two terms are absent. For illustration, we consider the case $Q = c$ and display the individual terms in $H_{\rm eff}$:

$$\begin{aligned}
H_{SS}^{(qq)} &= 2(\mathcal{K}_{cq})_{\bar{3}}[(\mathbf{S}_c \cdot \mathbf{S}_q) + (\mathbf{S}_{\bar{c}} \cdot \mathbf{S}_{\bar{q}})], \\
H_{SS}^{(q\bar{q})} &= 2(\mathcal{K}_{c\bar{q}})(\mathbf{S}_c \cdot \mathbf{S}_{\bar{q}} + \mathbf{S}_{\bar{c}} \cdot \mathbf{S}_q) + 2\mathcal{K}_{c\bar{c}}(\mathbf{S}_c \cdot \mathbf{S}_{\bar{c}}) + 2\mathcal{K}_{q\bar{q}}(\mathbf{S}_q \cdot \mathbf{S}_{\bar{q}}), \\
H_{SL} &= 2A_{\mathcal{Q}}(\mathbf{S}_{\mathcal{Q}} \cdot \mathbf{L} + \mathbf{S}_{\bar{\mathcal{Q}}} \cdot \mathbf{L}), \\
H_{LL} &= B_{\mathcal{Q}} \tfrac{L_{\mathcal{Q}\bar{\mathcal{Q}}}(L_{\mathcal{Q}\bar{\mathcal{Q}}}+1)}{2}.
\end{aligned} \tag{4}$$

Here $(\mathcal{K}_{cq})_{\bar{3}}$ parametrizes the spin-spin interaction between the charm c and the light quark q within a diquark in a color anti-triplet configuration, and the $(\mathcal{K}_{i\bar{j}}$ parametrize the spin-spin strengths between the quarks i and the antiquark $\bar{j}$, in the color-singlet configuration involving two different diquarks. The parameters $A_{\mathcal{Q}}$ and $B_{\mathcal{Q}}$ characterize the strength of the spin-orbit and the orbital angular force, respectively.
The usual angular momentum algebra then yields the following form:

$$\begin{aligned}
H_{\rm eff} &= 2m_{\mathcal{Q}} + \frac{B_{\mathcal{Q}}}{2}\langle L^2\rangle - 2a\langle L\cdot S\rangle + 2\kappa_{qc}\big[\langle s_q \cdot s_c\rangle + \langle s_{\bar{q}} \cdot s_{\bar{c}}\rangle\big] \\
&= 2m_{\mathcal{Q}} - aJ(J+1) + \left(\frac{B_{\mathcal{Q}}}{2} + a\right)L(L+1) + aS(S+1) - 3\kappa_{qc} \\
&\quad + \kappa_{qc}\big[s_{qc}(s_{qc}+1) + s_{\bar{q}\bar{c}}(s_{\bar{q}\bar{c}}+1)\big].
\end{aligned} \tag{5}$$

The effective Hamiltonian given above can be used for the tetraquark states involving a $b\bar{b}$ pair, with appropriate rescaling of the parameters.

Table 1: S-wave tetraquark states involving a $Q\bar{Q}$ pair in the two bases and their masses in the diquark model.

Label	J^{PC}	$\|s_{qQ}, s_{\bar{q}\bar{Q}}; S, L\rangle_J$	$\|s_{q\bar{q}}, s_{Q\bar{Q}}; S', L'\rangle_J$	Mass
X_0	0^{++}	$\|0,0;0,0\rangle_0$	$\big(\|0,0;0,0\rangle_0 + \sqrt{3}\|1,1;0,0\rangle_0\big)/2$	$M_{00} - 3\kappa_{qQ}$
X_0'	0^{++}	$\|1,1;0,0\rangle_0$	$\big(\sqrt{3}\|0,0;0,0\rangle_0 - \|1,1;0,0\rangle_0\big)/2$	$M_{00} + \kappa_{qQ}$
X_1	1^{++}	$\big(\|1,0;1,0\rangle_1 + \|0,1;1,0\rangle_1\big)/\sqrt{2}$	$\|1,1;1,L'\rangle_1$	$M_{00} - \kappa_{qQ}$
Z	1^{+-}	$\big(\|1,0;1,0\rangle_1 - \|0,1;1,0\rangle_1\big)/\sqrt{2}$	$\big(\|1,0;1,L'\rangle_1 - \|0,1;1,L'\rangle_1\big)/\sqrt{2}$	$M_{00} - \kappa_{qQ}$
Z'	1^{+-}	$\|1,1;1,0\rangle_1$	$\big(\|1,0;1,L'\rangle_1 + \|0,1;1,L'\rangle_1\big)/\sqrt{2}$	$M_{00} + \kappa_{qQ}$
X_2	2^{++}	$\|1,1;2,0\rangle_2$	$\|1,1;2,L'\rangle_2$	$M_{00} + \kappa_{qQ}$

Table 2: P-wave ($J^{PC} = 1^{--}$) tetraquark states involving a $Q\bar{Q}$ pair in the two bases and their masses in the diquark model.

Label	$\|s_{qQ}, s_{\bar{q}\bar{Q}}; S, L\rangle_J$	$\|s_{q\bar{q}}, s_{Q\bar{Q}}; S', L'\rangle_J$	Mass
Y_1	$\|0,0;0,1\rangle_1$	$\big(\|0,0;0,1\rangle_1 + \sqrt{3}\|1,1;0,1\rangle_1\big)/2$	$M_{00} - 3\kappa_{qQ} + B_Q$
Y_2	$\big(\|1,0;1,1\rangle_1 + \|0,1;1,1\rangle_1\big)/\sqrt{2}$	$\|1,1;1,L'\rangle_1$	$M_{00} - \kappa_{qQ} + 2a + B_Q$
Y_3	$\|1,1;0,1\rangle_1$	$\big(\sqrt{3}\|0,0;0,1\rangle_1 - \|1,1;0,1\rangle_1\big)/2$	$M_{00} + \kappa_{qQ} + B_Q$
Y_4	$\|1,1;2,1\rangle_1$	$\|1,1;2,L'\rangle_1$	$M_{00} + \kappa_{qQ} + 6a + B_Q$
Y_5	$\|1,1;2,3\rangle_1$	$\|1,1;2,L'\rangle_1$	$M_{00} + \kappa_{qQ} + 16a + 6B_Q$

3.2 Low-lying S and P-wave tetraquark states in the $c\bar{c}$ and $b\bar{b}$ sectors

The states in the diquark-antidiquark basis $|s_{qQ}, s_{\bar{q}\bar{Q}}; S, L\rangle_J$ and in the $Q\bar{Q}$ and $q\bar{q}$ basis $|s_{q\bar{q}}, s_{Q\bar{Q}}; S', L'\rangle_J$ are related by Fierz transformation. The positive parity S-wave tetraquarks are given in terms of the six states listed in Table 1 (charge conjugation is defined for neutral states). These states are characterized by the quantum number $L = 0$, hence their masses depend on just two parameters M_{00}, the diquark mass, and κ_{qQ}, leading to several predictions to be tested against experiments. The P-wave states are listed in Table 2. The first four of them have $L = 1$, and the fifth has $L = 3$, and hence is expected to be significantly heavier.
The parameters appearing on the r.h. columns of Tables 1 and 2 can be determined using the masses of some of the observed X, Y, Z states, and their numerical values are given in Table 3. Some parameters in the $c\bar{c}$ and $b\bar{b}$ sectors can also be related using the heavy quark mass scaling [53].
Typical errors on the masses due to parametric uncertainties are estimated to be about 30 MeV. Of course, this assumes that the effective Hamiltonian framework is a good approximation, and the error from this assumption is hard to quantify. There are several predictions in the charmonium-like sector, which, with the values of the parameters given in the tables above, are in the right ball-park [2]. It should be remarked that these input values, in particular for the quark-quark couplings in a diquark, κ_{qQ}, are larger than in the earlier determinations by Maiani *et al.* [32].In the modified scheme [42], the parameters ($\kappa_{i\bar{j}}$ are set to zero, eliminating the $H_{SS}^{(q\bar{q})}$ term in the effective Hamiltonian. With this, better agreement is reached with experiments

[2] I thank Satoshi Mishima for providing these estimates.

Table 3: Numerical values of the parameters in $H_{\rm eff}$, obtained using some of the S and P-wave tetraquarks as input.

	charmonium-like	bottomonium-like
M_{00} [MeV]	3957	10630
κ_{qQ} [MeV]	67	23
B_Q [MeV]	268	329
a [MeV]	52.5	26

Table 4: X, Y, Z hadron masses from experiments and in the diquark-model.

		charmonium-like		bottomonium-like	
Label	J^{PC}	State	Mass [MeV]	State	Mass [MeV]
X_0	0^{++}	—	3756	—	10562
X_0'	0^{++}	—	4024	—	10652
X_1	1^{++}	$X(3872)$	3890	—	10607
Z	1^{+-}	$Z_c^+(3900)$	3890	$Z_b^{+,0}(10610)$	10607
Z'	1^{+-}	$Z_c^+(4020)$	4024	$Z_b^+(10650)$	10652
X_2	2^{++}	—	4024	—	10652
Y_1	1^{--}	$Y(4008)$	4024	$Y_b(10891)$	10891
Y_2	1^{--}	$Y(4260)$	4263	$Y_b(10987)$	10987
Y_3	1^{--}	$Y(4290)$ (or $Y(4220)$)	4292	—	10981
Y_4	1^{--}	$Y(4630)$	4607	—	11135
Y_5	1^{--}	—	6472	—	13036

assuming that diquarks are more tightly bound than suggested from the analysis of the baryons in the diquark-quark picture. Despite this success, the continued experimental absence of the two lowest-lying 0^{++} states, called X_0 and X_0', is puzzling. Perhaps, they are below the threshold for strong decays and decay weakly, and thus have not been looked for. Alternative calculations of the tetraquark spectrum based on diquark-antidiquark model have been carried out in other phenomenological schemes [54], and in the QCD sum rule framework [55, 56]. All of them share the common feature with the effective Hamiltonian approach discussed here, namely they anticipate a very rich tetraquark spectroscopy. So, if the diquark picture has come to stay, some dynamical selection rules are required to better understand the observed spectrum.

The exotic bottomonium-like states are currently rather sparse. The reason for this is that quite a few exotic candidates charmonium-like states were observed in the decays of B-hadrons. This mode is obviously not available for the hidden $b\bar{b}$ states. They can only be produced in hadro- and electroweak high energy processes. Tetraquark states with a single b quark can, in principle, also be produced in the decays of the B_c mesons, as pointed out recently [57]. As the $c\bar{c}$ and $b\bar{b}$ cross-section at the LHC are very large, we anticipate that the exotic spectroscopy involving the open and hidden heavy quarks is an area where significant new results will be reported by all the LHC experiments. Measurements of the production and decays of exotica, such as transverse-momentum distributions and polarization information, will go a long way in understanding the underlying dynamics.

As a side remark, we mention that recently there has been a lot of excitement due to the D0 observation [58] of a narrow structure $X(5568)$, consisting of four different quark flavors ($bdus$), found through the $B_s^0\pi^\pm$ decay mode. However, this has not been confirmed by the LHCb collaboration [59], despite the fact that LHCb has 20 times larger B_s^0 sample than that of D0. This would have been the first discovery of an open b-quark tetraquark state. They are anticipated in the compact tetraquark picture [57], and also in the hadron molecule framework [60].

We now discuss the three observed exotic states in the bottomonium sector in detail. The hidden $b\bar{b}$ state $Y_b(10890)$ with $J^{\rm P}=1^{--}$ was discovered by Belle in 2007 [61] in the process $e^+e^-\to Y_b(10890)\to(\Upsilon(1S),\Upsilon(2S),\Upsilon(3S))\pi^+\pi^-$ just above the $\Upsilon(5S)$. The branching ratios measured are about two orders of magnitude larger than anticipated from similar dipionic transitions in the lower $\Upsilon(nS)$ states and in the ψ' (for a review and references to earlier work, see Brambilla *et al* [62]). Also the dipion invariant mass distributions in the decays of Y_b are marked by the presence of the resonances $f_0(980)$ and $f_2(1270)$. This state was interpreted as a $J^{\rm PC}=1^{--}$ P-wave tetraquark [43, 44]. Subsequent to this, a Van Royen-Weiskopf formalism was used [45] in which direct electromagnetic couplings with the diquark-antidiquark pair of the Y_b was assumed. Due to the P-wave nature of the $Y_b(10890)$, with a commensurate small overlap function, the observed small production cross-section in $e^+e^-\to b\bar{b}$ is expected. In the tetraquark picture, the $Y_b(10890)$ is the $b\bar{b}$ analogue of the $c\bar{c}$ state $Y_c(4260)$, also a P-wave, which is likewise found to have a very small production cross-section, but decays readily into $J/\psi\pi^+\pi^-$. Hence, the two have very similar production and decay characteristics.

The current status of $Y_b(10890)$ is, however, unclear. Subsequent to its discovery, Belle undertook high-statistics scans to measure the ratio $R_{b\bar{b}}=\sigma(e^+e^-\to b\bar{b})/\sigma(e^+e^-\to\mu^+\mu^-)$, and also more precisely the ratios $R_{\Upsilon(nS)\pi^+\pi^-}=\sigma(e^+e^-\to\Upsilon(nS)\pi^+\pi^-)/\sigma(e^+e^-\to\mu^+\mu^-)$. They are shown in Fig. 6 and Fig. 7, respectively. The two masses, $M(5S)_{b\bar{b}}$ measured through $R_{b\bar{b}}$, and $M(Y_b)$, measured through $R_{\Upsilon(nS)\pi^+\pi^-}$, now differ by slightly more than 2σ, $M(5S)_{b\bar{b}}-M(Y_b)=-9\pm4$ MeV. From the mass difference alone, these two could very well be just one and the same state, namely the canonical $\Upsilon(5S)$ - an interpretation adopted by the Belle

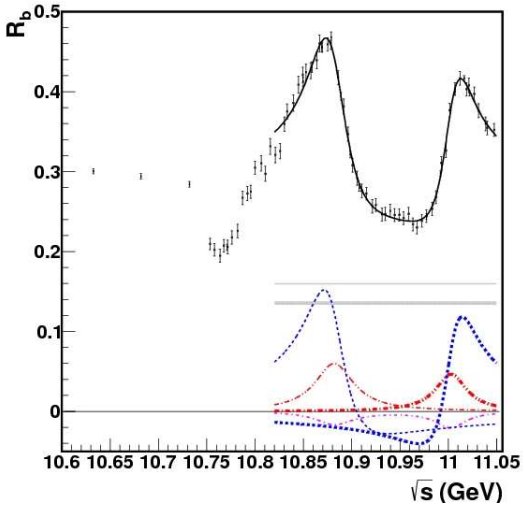

Figure 6: The ratio $R_b = \sigma(e^+e^- \to b\bar{b})/\sigma(e^+e^- \to \mu^+\mu^-)$ in the $Y(10860)$ and $Y(11020)$ region. The components of the fit are depicted in the lower part of the figure: total (solid curve), constant $|A_{ic}|^2$ (thin), $|A_c|^2$ (thick): for $\Upsilon(5S)$ (thin) and $\Upsilon(6S)$ (thick): $|f|^2$ (dot-dot-dash), cross terms with A_c (dashed), and two-resonance cross term (dot-dash). Here, A_c and A_{ic} are coherent and incoherent continuum terms, respectively (from Belle [63]).

collaboration [63]. On the other hand, it is now the bookkeeping of the branching ratios measured at or near the $\Upsilon(5S)$, which is puzzling. This is reflected in the paradox that *direct production* of the $B^{(*)}\bar{B}^{(*)}$ as well as of $B_s\bar{B}_s^{(*)}$ states have essentially no place in the Belle accounting [63], even though these reactions have measured cross sections, first observed by CLEO [74]. The branching ratios of the $\Upsilon(5S)$ measured by Belle are already saturated by the exotic states $(\Upsilon(nS)\pi^+\pi^-, h_b(mP)\pi^+\pi^-, Z_b(10610)^\pm\pi^\mp, Z_b(10650)^\pm\pi^\mp$ and their isospin partners). The reason for this mismatch is not clear, and is attributed by Belle to the inadequate modeling of R_b due to several thresholds in this energy reason. In our opinion, an interpretation of the Belle data based on two resonances $\Upsilon(5S)$ and $Y_b(10890)$ is more natural, with $\Upsilon(5S)$ having the decays expected for the bottomonium S-state above the $B^{(*)}\bar{B}^{(*)}$ threshold, and the decays of $Y_b(10890)$, a tetraquark, being the source of the exotic states seen. As data taking starts in a couple of years in the form of a new and expanded collaboration, Belle-II, cleaning up the current analysis in the $\Upsilon(5S)$ and $\Upsilon(6S)$ region should be one of their top priorities.

Thus, the hypothesis that $\Upsilon(5S)$ and $Y_b(10890)$, while having the same $J^{\rm PC} = 1^{--}$ quantum numbers and almost the same mass, are *different* states, is still not completely ruled out. As already mentioned, this is hinted by the drastically different decay characteristics of the dipionic transitions involving the lower quarkonia S-states, such as $\Upsilon(4S) \to \Upsilon(1S)\pi^+\pi^-$, on one hand, and similar decays of the Y_b, on the other. These anomalies are seen both in the decay rates and in the dipion invariant mas spectra in the $\Upsilon(nS)\pi^+\pi^-$ modes. The large branching ratios of $Y_b \to \Upsilon(nS)\pi^+\pi^-$, as well as of $Y(4260) \to J/\psi\pi^+\pi^-$, are due to the Zweig-allowed nature of these transitions, as the initial and final states have the same valence quarks. The final state $\Upsilon(nS)\pi^+\pi^-$ in Y_b decays requires the excitation of a $q\bar{q}$ pair from the vacuum. Since, the light scalars σ_0, $f_0(980)$ are themselves tetraquark candidates [64, 65], they are expected to show

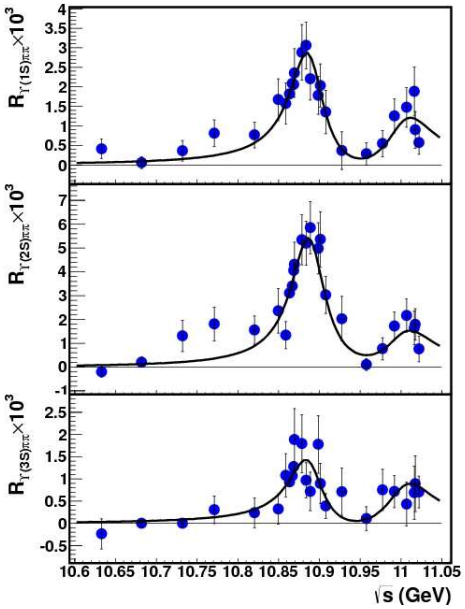

Figure 7: The ratio $R_{\Upsilon(nS)\pi^+\pi^-} = \sigma(e^+e^- \to \Upsilon(nS)\pi^+\pi^-)/\sigma(e^+e^- \to \mu^+\mu^-)$ in the $Y(10860)$ and $Y(11020)$ region (from Belle [63]).

up in the $\pi^+\pi^-$ invariant mass distributions, as opposed to the corresponding spectrum in the transition $\Upsilon(4S) \to \Upsilon(1S)\pi^+\pi^-$ (see Fig. 8). Subsequent discoveries [66] of the charged states $Z_b^+(10610)$ and $Z_b^+(10650)$, found in the decays $\Upsilon(5S)/Y_b \to Z_b^+(10610)\pi^-, Z_b^+(10650)\pi^-$, leading to the final states $\Upsilon(1S)\pi^+\pi^-$, $\Upsilon(2S)\pi^+\pi^-$, $\Upsilon(3S)\pi^+\pi^-$, $h_b(1P)\pi^+\pi^-$ and $h_b(2P)\pi^+\pi^-$, give credence to the tetraquark interpretation, as discussed below.

3.3 Heavy-Quark-Spin Flip in $\Upsilon(10890) \to h_b(1P, 2P)\pi\pi$

The cross-section $\sigma(e^+e^- \to (h_b(1P), h_b(2P)\pi^+\pi^-)$ measured by Belle [67] is shown in Fig. 9, providing clear evidence of the production in the $\Upsilon(10860)$ and $\Upsilon(11020)$ region. We summarize the relative rates and strong phases measured by Belle [66] in the process $\Upsilon(10890) \to \Upsilon(nS)\pi^+\pi^-, h_b(mP)\pi^+\pi^-$, with $n = 1, 2, 3$ and $m = 1, 2$ in Table 5. For ease of writing we shall use the notation Z_b and Z_b' for the two charged Z_b states. Here no assumption is made about the nature of $\Upsilon(10890)$, it can be either $\Upsilon(5S)$ or Y_b. Of these, the decay $\Upsilon(10890) \to \Upsilon(1S)\pi^+\pi^-$ involves both a resonant (i.e., via Z/Z') and a direct component, but the other four are dominated by the resonant contribution. One notices that the relative normalizations are very similar and the phases of the $(\Upsilon(2S), \Upsilon(3S))\pi^+\pi^-$ differ by about 180° compared to the ones in $(h_b(1P, h_b(2P))\pi^+\pi^-$. At the first sight this seems to violate the heavy-quark-spin conservation, as in the initial state $s_{b\bar{b}} = 1$, which remains unchanged for the $\Upsilon(nS)$ in the final state, i.e., it involves an $s_{b\bar{b}} = 1 \to s_{b\bar{b}} = 1$ transition, but as $s_{b\bar{b}} = 0$ for the $h_b(mP)$, this involves an $s_{b\bar{b}} = 1 \to s_{b\bar{b}} = 0$ transition, which should have been suppressed, but is not supported by data. It has been shown that this contradiction is only apparent [53]. Expressing the states Z_b and Z_b' in the basis of definite $b\bar{b}$ and light quark $q\bar{q}$ spins, it becomes evident that both the Z_b and

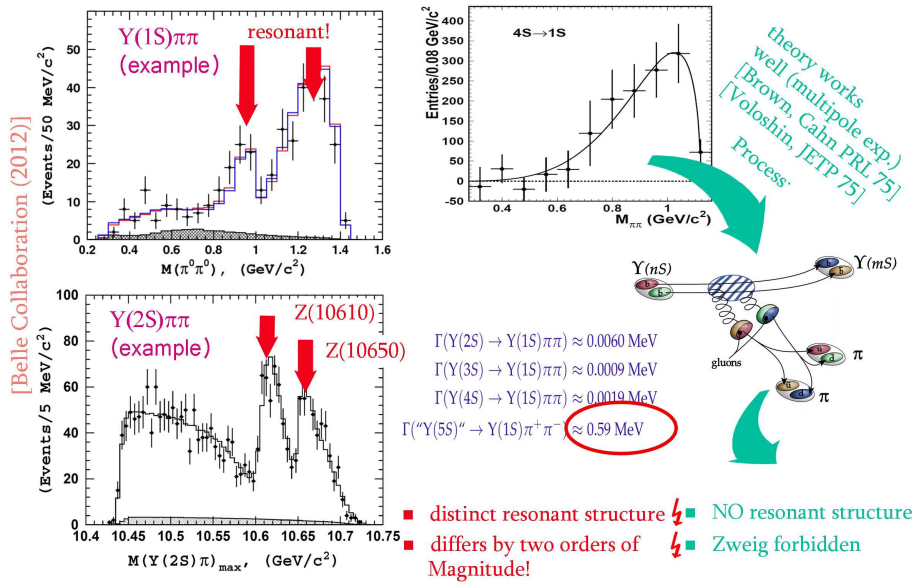

Figure 8: Dipion invariant mass distribution in $\Upsilon(10890) \to \Upsilon(1S)\pi^0\pi^0$ (upper left frame); the resonances indicated in the dipion spectrum correspond to the $f_0(980)$ and $f_2(1270)$; the resonances $Z(10610)$ and $Z(10650)$ are indicated in the $\Upsilon(2S)\pi^+$ invariant mass distribution from $\Upsilon(10890) \to \Upsilon(2S)\pi^+\pi^-$ (lower left frame). The data are from the Belle collaboration [66]. The upper right hand frame shows the dipion invariant mass distribution in $\Upsilon(4S) \to \Upsilon(1S)\pi^+\pi^-$, and the theoretical curve (with the references) is based on the Zweig-forbidden process shown below. The measured decay widths from $\Upsilon(nS) \to \Upsilon(1S)\pi^+\pi^-$ $nS = 2S, 3S, 4S$ and $\Upsilon(10890) \to \Upsilon(1S)\pi^+\pi^-$ are also shown.

Table 5: Relative normalizations and phases for $s_{b\bar{b}} : 1 \to 1$ and $1 \to 0$ transitions in $\Upsilon(10890)$ decays [66].

Final State	$\Upsilon(1S)\pi^+\pi^-$	$\Upsilon(2S)\pi^+\pi^-$	$\Upsilon(3S)\pi^+\pi^-$	$h_b(1P)\pi^+\pi^-$	$h_b(2P)\pi^+\pi^-$
Rel. Norm.	$0.57 \pm 0.21^{+0.19}_{-0.04}$	$0.86 \pm 0.11^{+0.04}_{-0.10}$	$0.96 \pm 0.14^{+0.08}_{-0.05}$	$1.39 \pm 0.37^{+0.05}_{-0.15}$	$1.6^{+0.6+0.4}_{-0.4-0.6}$
Rel. Phase	$58 \pm 43^{+4}_{-9}$	$-13 \pm 13^{+17}_{-8}$	$-9 \pm 19^{+11}_{-26}$	187^{+44+3}_{-57-12}	$181^{+65+74}_{-105-109}$

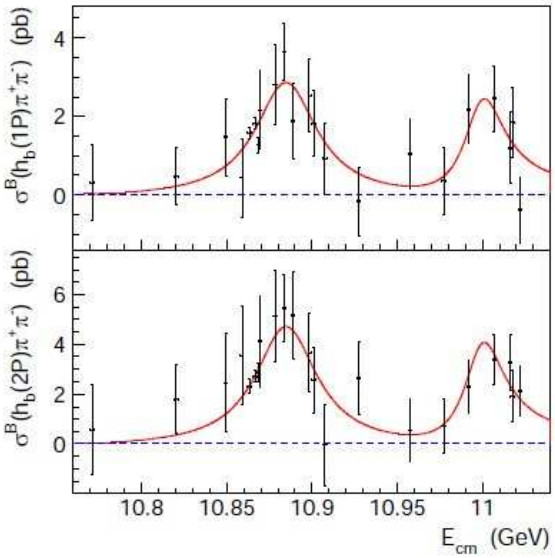

Figure 9: $\sigma(e^+e^- \to h_b(1P)\pi^+\pi^-)$ and $\sigma(e^+e^- \to h_b(2P)\pi^+\pi^-)$-in the $Y(10860)$ and $Y(11020)$ region(from Belle [67]).

Z_b' have $s_{b\bar{b}} = 1$ and $s_{b\bar{b}} = 0$ components,

$$|Z_b\rangle = \frac{|1_{q\bar{q}}, 0_{b\bar{b}}\rangle - |0_{q\bar{q}}, 1_{b\bar{b}}\rangle}{\sqrt{2}}, \quad |Z_b'\rangle = \frac{|1_{q\bar{q}}, 0_{b\bar{b}}\rangle + |0_{q\bar{q}}, 1_{b\bar{b}}\rangle}{\sqrt{2}} \tag{6}$$

Defining (g is the effective couplings at the vertices $\Upsilon\, Z_b\, \pi$ and $Z_b\, h_b\, \pi$)

$$\begin{aligned} g_Z &\equiv g(\Upsilon \to Z_b\pi)g(Z_b \to h_b\pi) \propto -\alpha\beta\langle h_b|Z_b\rangle\langle Z_b|\Upsilon\rangle, \\ g_{Z'} &\equiv g(\Upsilon \to Z_b'\pi)g(Z_b' \to h_b\pi) \propto \alpha\beta\langle h_b|Z_b'\rangle\langle Z_b'|\Upsilon\rangle, \end{aligned} \tag{7}$$

we note that within errors, Belle data is consistent with the heavy quark spin conservation, which requires $g_Z = -g_{Z'}$. The two-component nature of the Z_b and Z_b' is also the feature which was pointed out earlier for Y_b in the context of the direct transition $Y_b(10890) \to \Upsilon(1S)\pi^+\pi^-$. To determine the coefficients α and β, one has to resort to $s_{b\bar{b}}$: $1 \to 1$ transitions

$$\Upsilon(10890) \to Z_b/Z_b' + \pi \to \Upsilon(nS)\pi\pi \ (n = 1, 2, 3). \tag{8}$$

The analogous effective couplings are

$$\begin{aligned} f_Z &= f(\Upsilon \to Z_b\pi)f(Z_b \to \Upsilon(nS)\pi) \propto |\beta|^2\langle\Upsilon(nS)|0_{q\bar{q}}, 1_{b\bar{b}}\rangle\langle 0_{q\bar{q}}, 1_{b\bar{b}}|\Upsilon\rangle, \\ f_{Z'} &= f(\Upsilon \to Z_b'\pi)f(Z_b' \to \Upsilon(nS)\pi) \propto |\alpha|^2\langle\Upsilon(nS)|0_{q\bar{q}}, 1_{b\bar{b}}\rangle\langle 0_{q\bar{q}}, 1_{b\bar{b}}|\Upsilon\rangle. \end{aligned} \tag{9}$$

Dalitz analysis indicates that $\Upsilon(10890) \to Z_b/Z_b' + \pi \to \Upsilon(nS)\pi\pi$ $(n = 1, 2, 3)$ proceed mainly through the resonances Z_b and Z_b', though $\Upsilon(10890) \to \Upsilon(1S)\pi\pi$ has a significant direct component, expected in tetraquark interpretation of $\Upsilon(10890)$ [45]. A comprehensive analysis of

the Belle data including the direct and resonant components is required to test the underlying dynamics, which yet to be carried out. However, parametrizing the amplitudes in terms of two Breit-Wigners, one can determine the ratio α/β from $\Upsilon(10890) \to Z_b/Z_b' + \pi \to \Upsilon(nS)\pi\pi$ ($n = 1, 2, 3$). For the $s_{b\bar{b}} : 1 \to 1$ transition, we get for the averaged quantities:

$$\overline{\text{Rel.Norm.}} = 0.85 \pm 0.08 = |\alpha|^2/|\beta|^2; \quad \overline{\text{Rel.Phase}} = (-8 \pm 10)^\circ. \tag{10}$$

For the $s_{b\bar{b}} : 1 \to 0$ transition, we get

$$\overline{\text{Rel.Norm.}} = 1.4 \pm 0.3; \quad \overline{\text{Rel.Phase}} = (185 \pm 42)^\circ. \tag{11}$$

Within errors, the tetraquark assignment with $\alpha = \beta = 1$ is supported, i.e.,

$$|Z_b\rangle = \frac{|1_{bq}, 0_{\bar{b}\bar{q}}\rangle - |0_{bq}, 1_{\bar{b}\bar{q}}\rangle}{\sqrt{2}}, \quad |Z_b'\rangle = |1_{bq}, 1_{\bar{b}\bar{q}}\rangle_{J=1}, \tag{12}$$

and

$$|Z_b\rangle = \frac{|1_{q\bar{q}}, 0_{b\bar{b}}\rangle - |0_{q\bar{q}}, 1_{b\bar{b}}\rangle}{\sqrt{2}}, \quad |Z_b'\rangle = \frac{|1_{q\bar{q}}, 0_{b\bar{b}}\rangle + |0_{q\bar{q}}, 1_{b\bar{b}}\rangle}{\sqrt{2}}. \tag{13}$$

It is interesting that similar conclusion was drawn in the 'molecular' interpretation [68] of the Z_b and Z_b'.
The Fierz rearrangement used in obtaining second of the above relations would put together the $b\bar{q}$ and $q\bar{b}$ fields, yielding

$$|Z_b\rangle = |1_{b\bar{q}}, 1_{\bar{b}q}\rangle_{J=1}, \quad |Z_b'\rangle = \frac{|1_{b\bar{q}}, 0_{q\bar{b}}\rangle + |0_{b\bar{q}}, 1_{q\bar{b}}\rangle}{\sqrt{2}}. \tag{14}$$

Here, the labels $0_{b\bar{q}}$ and $1_{\bar{q}b}$ could be viewed as indicating B and B^* mesons, respectively, leading to the prediction $Z_b \to B^*\bar{B}^*$ and $Z_b' \to B\bar{B}^*$, which is not in agreement with the Belle data [66]. However, this argument rests on the conservation of the light quark spin, for which there is no theoretical foundation. Hence, this last relation is not reliable. Since $Y_b(10890)$ and $\Upsilon(5S)$ are rather close in mass, and there is an issue with the unaccounted *direct production* of the $B^*\bar{B}^*$ and $B\bar{B}^*$ states in the Belle data collected in their vicinity, we conclude that the experimental situation is still in a state of flux and look forward to its resolution with the consolidated Belle-II data.

The exotic hadrons having $J^{\rm PC} = 1^{--}$ can be produced at the Tevatron and LHC via the Drell-Yan process [69] $pp(\bar{p}) \to \gamma^* \to V + ...$ The cases $V = \phi(2170), Y(4260), Y_b(10890)$ have been studied [69]. With the other two hadrons already discussed earlier, we recall that $\phi(2170)$ was first observed in the ISR process $e^+e^- \to \gamma_{\rm ISR} f_0(980)\phi(1020)$ by BaBaR [70] and later confirmed by BESII [71] and Belle [72]. Drenska *et al.* [73] interpreted $\phi(1270)$ as a P-wave tetraquark $[sq][\bar{s}\bar{q}]$. Thus, all three vector exotica are assumed to be the first orbital excitation of diquark-antidiquark states with a hidden $s\bar{s}$, $c\bar{c}$ and $b\bar{b}$ quark content, respectively. As all three have very small branching ratios in a dilepton pair, they should be searched for in the decay modes in which they have been discovered, and these are $\phi(2170) \to f_0(980)\phi(1020) \to \pi^+\pi^-K^+K^-$, $Y(4260) \to J/\psi\pi^+\pi^- \to \mu^+\mu^-\pi^+\pi^-$ and $Y_b(10890) \to \Upsilon(nS)\pi^+\pi^- \to \mu^+\mu^-\pi^+\pi^-$. Thus, they involve four charged particles, which can be detected at hadron colliders. The cross sections for the processes $p\bar{p}(p) \to \phi(2170)(\to \phi(1020)f_0(980) \to$

$K^+K^-\pi^+\pi^-$), $p\bar{p}(p) \to Y(4260)(\to J/\psi\pi^+\pi^- \to \mu^+\mu^-\pi^+\pi^-)$, and $p\bar{p}(p) \to Y_b(10890)(\to \Upsilon(1S,2S,3S)\pi^+\pi^- \to \mu^+\mu^-\pi^+\pi^-)$, at the Tevatron ($\sqrt{s} = 1.96$ TeV) and the LHC are computed in [69]. All these processes have measurable rates, and they should be searched for at the LHC.

Summarizing the tetraquark discussion, we note that there are several puzzles in the X, Y, Z sector, and the underlying dynamics is not understood. Apart from the rich spectrum in the diquark scenario and the continued absence of many predicted states, they involve the nature of the observed states $J^{PC} = 1^{--}$, $Y(4260)$ and $Y(10890)$, and whether they are related with each other. Also, whether $Y(10890)$ and $\Upsilon(5S)$ are one and the same particle is still an open issue. In principle, both $Y(4260)$ and $Y(10890)$ can be produced at the LHC and measured through the $J\psi\pi^+\pi^-$ and $\Upsilon(nS)\pi^+\pi^-$ ($nS = 1S, 2S, 3S$) modes, respectively. Their hadroproduction cross-sections are unfortunately uncertain, but their (normalized) transverse momentum distributions will be quite revealing. As they are both $J^{PC} = 1^{--}$ hadrons, they can also be produced via the Drell-Yan mechanism and detected through their signature decay modes. The tetraquark interpretation of the charged exotics Z_b and Z_b' leads to a straight forward understanding of the relative rates and strong phases of the heavy quark spin non-flip and spin-flip transitions in the decays $\Upsilon(10890) \to \Upsilon(nS)\pi^+\pi^-$ and $\Upsilon(10890) \to h_b(mP)\pi^+\pi^-$, respectively. In the tetraquark picture, the corresponding hadrons in the charm sector Z_c and Z_c' are related to their $b\bar{b}$ counterparts.

4 Pentaquarks

Pentaquarks remained elusive for almost a decade under the shadow of the botched discoveries of $\Theta(1540)$, $\Phi(1860)$, $\Theta_c(3100)$. The sentiment of the particle physics community is reflected in the terse 2014 PDG review [75], which characterizes them as false alarms. This has definitely changed by the observation of $J/\psi p$ resonances consistent with pentaquark states in $\Lambda_b^0 \to J/\psi K^- p$ decays by the LHCb collaboration [2]:

$$pp \to b\bar{b} \to \Lambda_b X; \Lambda_b \to K^- J/\psi p. \tag{15}$$

The measured distributions in the invariant masses m_{Kp} and $m_{J/\psi p}$ are shown in Fig. 10 together with a model comparison with two P_c^+ states. A statistically good fit of the $m_{J/\psi p}$ distribution is consistent with the presence of two resonant states, henceforth called $P_c(4450)^+$ and $P_c(4380)^+$, with the following characteristics

$$M = 4449.8 \pm 1.7 \pm 2.5 \text{ MeV}; \quad \Gamma = 39 \pm 5 \pm 19 \text{ MeV}, \tag{16}$$

and

$$M = 4380 \pm 8 \pm 29 \text{ MeV}; \quad \Gamma = 205 \pm 18 \pm 86 \text{ MeV}. \tag{17}$$

Both of these states carry a unit of baryonic number and have the valence quarks $P_c^+ = \bar{c}cuud$. The preferred $J^{\rm P}$ assignments are $5/2^+$ for the $P_c(4450)^+$ and $3/2^-$ for the $P_c(4380)^+$.

Doing an Argand-diagram analysis in the (Im A^{P_c} - Re A^{P_c}) plane, the phase change in the amplitude is consistent with a resonance for the $P_c(4450)^+$, but less so for the $P_c(4380)^+$, as shown in Fig. 11. The phase diagram for the $P_c(4380)^+$ state needs further study with more data, but the resonant character of the $P_c(4450)^+$ state is established beyond doubt. This will be contrasted with the corresponding phase diagram resulting from the assumption that $P_c(4450)^+$ is a kinematically-induced cusp state.

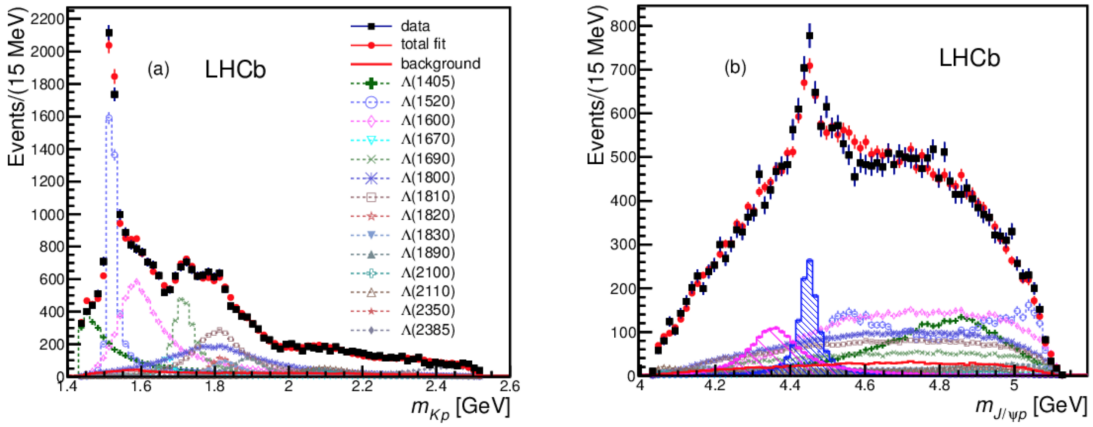

Figure 10: Fit projections for (a) m_{Kp} and (b) $m_{J/\psi p}$ distributions for the reduced Λ^* model with two P_c^+ states, $P_c(4450)$ blue (open) squares with shaded histogram and $P_c(4380)^+$ with (purple) filled squares. Each Λ^* component is also shown. (from LHCb [2]).

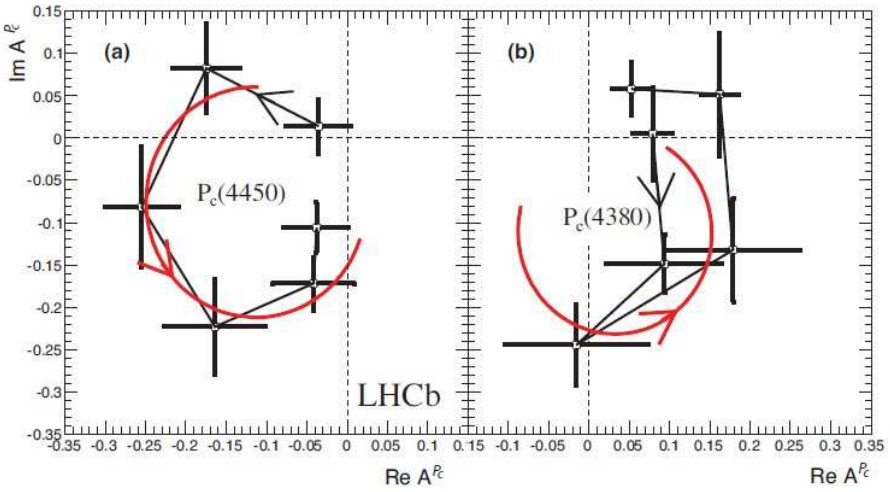

Figure 11: Fitted values of the real and imaginary parts of the amplitudes for the $(3/2^-, 5/2^+)$ assignments for (a) the $P_c(4450)^+$ state and (b) the $P_c(4380)^+$ state, each divided into six $m_{J/\psi p}$ bins of equal width between $-\Gamma$ and $+\Gamma$ shown in the Argand diagrams as connected points with error bars. The solid (red) curves are the predictions from the Breit-Wigner formula for the same mass range with $M(\Gamma)$ of 4450(39) MeV and 4380 (205) MeV, respectively. (from LHCb [2]).

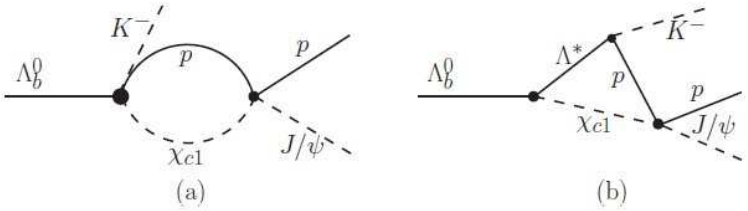

Figure 12: The two scattering diagrams discussed in the text [78].

Following a pattern seen for the tetraquark candidates, namely their proximity to respective thresholds, such as $D\bar{D}^*$ for the $X(3872)$, $B\bar{B}^*$ and $B^*\bar{B}^*$ for the $Z_b(10610)$ and $Z_b(10650)$, respectively, also the two pentaquark candidates $P_c(4380)$ and $P_c(4450)$ lie close to several charm meson-baryon thresholds [76]. The $\Sigma_c^{*+}\bar{D}^0$ has a threshold of 4382.3 ± 2.4 MeV, tantalizingly close to the mass of $P_c(4380)^+$. In the case of $P_c(4450)^+$, there are several thresholds within striking distance, $\chi_{c1}p(4448.93 \pm 0.07), \Lambda_c^{*+}\bar{D}^0(4457.09 \pm 0.35), \Sigma_c^+\bar{D}^{*0}(4459.9 \pm 0.9)$, and $\Sigma_c^+\bar{D}^0\pi^0(4452.7 \pm 0.5)$, where the masses are in units of MeV. This has led to a number of hypotheses to explain the two P_c states:

- $P_c(4380)$ and $P_c(4450)$ are baryocharmonia [77].
- Rescattering-induced kinematic effects are mimicking the resonances [78, 79, 80, 81].
- They are open charm-baryon and charm-meson bound states [82, 83, 84, 85, 86].
- They are compact diquark-diquark-antiquark states [87, 88, 89, 90, 91, 92, 93, 94], with each component being a $\bar{3}$, yielding a color-singlet $\bar{c}[cq][qq]$ state. Another possibility is via the sequential formation of compact color triplets, making up diquark-triquark systems, yielding also color-singlet states [95, 96].

In the baryocharmonium picture, the P_c states are hadroquarkonium-type composites of J/ψ and excited nucleon states similar to the known resonances $N(1440)$ and $N(1520)$. Photoproduction of the P_c states in $\gamma + p$ collisions is advocated as sensitive probe of this mechanism [77]. We shall discuss below the interpretation of pentaquarks as scattering-induced kinematic effects, and as meson-baryon molecules, but review the compact diquark-based models in quite some detail.

4.1 Pentaquarks as rescattering-induced kinematic effects

Kinematic effects can result in a narrow structure around the $\chi_{c1}p$ threshold. Two possible mechanisms shown in Fig. 12 are:
(a) 2-point loop with a 3-body production $\Lambda_b^0 \to K^-\,\chi_{c1}\,p$ followed by the rescattering process $\chi_{c1}\,p \to J/\psi\,p$, and
(b) in which $K^-\,p$ is produced from an intermediate Λ^* and the proton rescatters with the χ_{c1} into a $J/\psi\,p$, as shown below.

The amplitude for Fig. (a) can be expressed as

$$G_\Lambda(E) = \int \frac{d^3q}{(2\pi)^3} \frac{\vec{q}^2 f_\Lambda(\vec{q}^2)}{E - m_p - m_{\chi_{c1}} - \vec{q}^2/(2\mu)}, \tag{18}$$

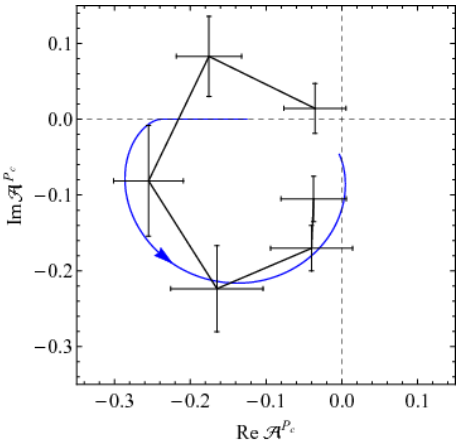

Figure 13: Fitted values of the real and imaginary parts of the amplitudes for the $P_c(4450)^+$ using a Breit-Wigner formula with $M(\Gamma)$ of 4450(39) MeV [2]. The directed curve (blue) is the fit in the cusp model. (from [78]).

where μ is the reduced mass and $f_\Lambda(\vec{q}^2) = \exp(-2\vec{q}^2/\Lambda^2)$ is a form factor to regularize the loop integral. Fitting the Argand diagram for the $P_c(4450)^+$ with $\mathcal{A}_{(a)} = N(b + G_\Lambda(E))$ determines the normalization N, the constant background b, and Λ. The integral can be solved analytically [78]

$$G_\Lambda(E) = \frac{\mu\Lambda}{(2\pi)^{3/2}}(k^2 + \Lambda^2/4) + \frac{\mu k^3}{2\pi}\exp^{-2k^2/\Lambda^2}\left[erfc(\frac{\sqrt{2}k}{\Lambda}) - i\right] \tag{19}$$

where $k = \sqrt{2\mu(E - m_1 - m_2 + i\epsilon)}$. This function has a characteristic phase motion reflecting the error function, as shown in Fig. 13. It differs from the Breit-Wigner fit, which is in excellent agreement with the LHCb data [2]. The cusp-based fit also shows a counter-clockwise behavior in the Argand diagram, but not for the two data points where the imaginary part of the cusp amplitude is zero. The absolute value of the amplitude in the cusp approach shows a resonant behavior, which can be made to peak even more sharply at $\mathrm{Re}\sqrt{s} = 4450$ MeV, if the amplitude for Fig. 12 (b) is included and assumed dominated by the $\Lambda^*(1890)$-exchange. However, it is the phase motion, which is decisive in distinguishing a dynamical Breit-Wigner (or, for that matter a Flatte [97] type) resonance and a kinematic-induced cusp behavior. More data is needed to completely settle this difference in the case of $P_c(4450)^+$, but currently the Breit-Wigner fit is the preferred description.

4.2 Pentaquarks as meson-baryon molecules

In the hadronic molecular interpretation, one identifies the $P_c(4380)^+$ with $\Sigma_c(2455)\bar{D}^*$ and the $P_c(4450)^+$ with $\Sigma_c(2520)\bar{D}^*$, which are bound by a pion exchange. The underlying interaction

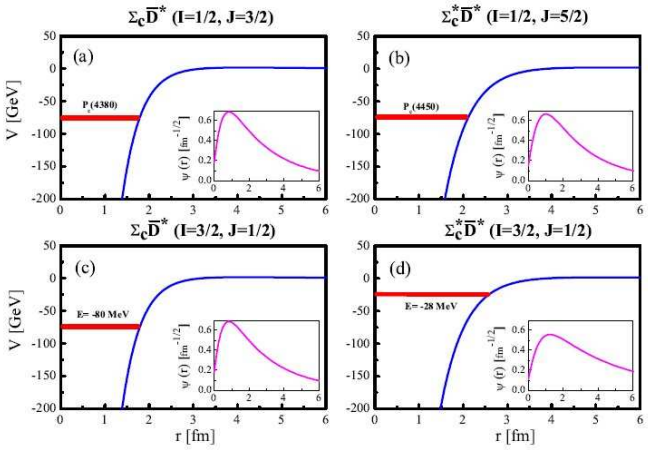

Figure 14: Effective potentials, V (GeV), energy levels, thick (red) lines, and wave-functions, $\psi(r)$, of the $\Sigma_c^{(*)}\bar{D}^*$ system (from [85]).

can be expressed in terms of the effective Lagrangians [85]:

$$\mathcal{L}_{\mathcal{P}} = ig\mathrm{Tr}\left[\bar{H}_a^{(\bar{Q})}\,\gamma^\mu\,A^\mu_{ab}\,\gamma_5 H_b^{(\bar{Q})}\right],$$
$$\mathcal{L}_{\mathcal{S}} = -\frac{3}{2}g_1\epsilon^{\mu\lambda\nu\kappa}v_\kappa\mathrm{Tr}\left[\bar{\mathcal{S}}_\mu\,A_\nu\,\mathcal{S}_\lambda\right], \qquad (20)$$

which are built using the heavy quark and chiral symmetries. Here $H_a^{(\bar{Q})} = [P_a^{*(\bar{Q})\,\mu}\gamma_\mu - P_a^{(\bar{Q})}\gamma_5](1-\not{v})/2$ is a pseudoscalar and vector charmed meson multiplet (D, D^*), v being the four-velocity vector $v = (0, \vec{1})$, $\mathcal{S}_\mu = 1/\sqrt{3}(\gamma_\mu + v_\mu)\gamma^5\mathcal{B}_6 + \mathcal{B}^*_{6\mu}$ stands for the charmed baryon multiplet, with $\mathcal{B}_6$ and $\mathcal{B}^*_{6\mu}$ corresponding to the $J^P = 1/2^+$ and $J^P = 3/2^+$ in 6_F flavor representation, respectively. A_μ is an axial-vector current, containing a pion chiral multiplet, defined as $A_\mu = 1/2(\xi^\dagger\partial_\mu\xi - \xi\partial_\mu\xi^\dagger)$, with $\xi = \exp(i\mathbb{P}/f_\pi)$, with $\mathbb{P}$ an $SU(2)$ matrix containing the pion field, and $f_\pi = 132$ MeV. This interaction Lagrangian is used to work out effective potentials, energy levels and wave-functions of the $\Sigma_c^{(*)}\bar{D}^*$ systems, shown in Fig. 14. In this picture, $P_c(4380)^+$ is a $\Sigma_c\bar{D}^*$ $(I = 1/2,\, J = 3/2)$ molecule, and $P_c(4450)^+$ is a $\Sigma_c^*\bar{D}^*$ $(I = 1/2,\, J = 5/2)$ molecule.

Apart from accommodating the two observed pentaquarks, this framework predicts two additional hidden-charm molecular pentaquark states, $\Sigma_c\bar{D}^*$ $(I = 3/2,\, J = 1/2)$ and $\Sigma_c^*\bar{D}^*$ $(I = 3/2,\, J = 1/2)$, which are isospin partners of $P_c(4380)^+$ and $P_c(4450)^+$, respectively, decaying into $\Delta(1232)J/\psi$ and $\Delta(1232)\eta_c$. In addition, a rich pentaquark spectrum of states for the hidden-bottom $(\Sigma_b B^*, \Sigma_b^* B^*)$, B_c-like $(\Sigma_c B^*, \Sigma_c^* B^*)$ and $(\Sigma_b\bar{D}^*, \Sigma_b^*\bar{D}^*)$ with well-defined (I, J) is predicted.

5 Pentaquarks in the compact diquark models

In the pioneering work by Maiani *et al.* [87] on the pentaquark interpretation of the LHCb data on $\Lambda_b^0 \to J/\psi\; p\; K^-$ decay, which is mainly discussed here, the assigned internal quantum numbers are: $P_c^+(4450) = \{\bar{c}[cu]_{s=1}[ud]_{s=0}; L_{\mathcal{P}} = 1, J^{\mathrm{P}} = \frac{5}{2}^+\}$ and $P_c^+(4380) = \{\bar{c}[cu]_{s=1}[ud]_{s=1}; L_{\mathcal{P}} =$

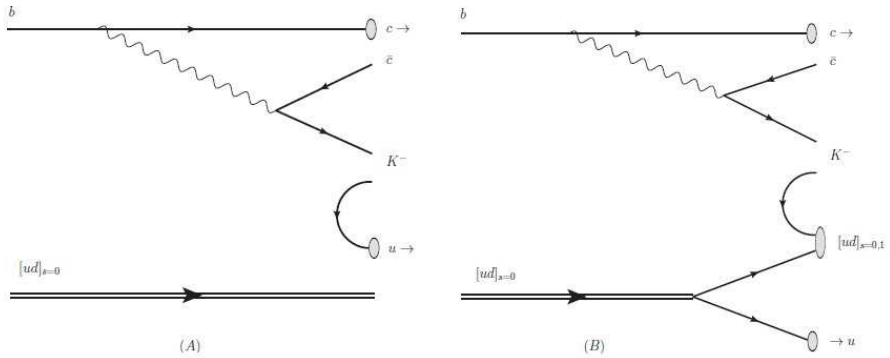

Figure 15: Two mechanisms for the decays $\Lambda_b^0 \to J/\psi K^- p$ in the pentaquark picture (from [87].

$0, J^{\rm P} = \frac{3}{2}^-\}$. Taking into account the mass differences due to the orbital angular momentum and the light diquark spins, the observed mass difference between the two P_c^+ states of about 70 MeV is reproduced. The crucial assumption is that the two diagrams for the decay $\Lambda_b^0 \to J/\psi\ p\ K^-$ in which the ud-spin in Λ_b^0 goes over to the $[ud]$-diquark spin in the pentaquark, Fig. 15(A), and the one in which the ud-spin is shared among the final state pentaquark and a meson, generating a light diquark $[ud]$ having spin-0 and spin-1, Fig. 15(B), are treated at par. This is a dynamical assumption, and remains to be tested.

5.1 $SU(3)_F$ structure of pentaquarks

Concentrating on the quark flavor of the pentaquarks $\mathbb{P}_c^+ = \bar{c}cuud$, they are of two different types [87]:

$$\mathbb{P}_u = \epsilon^{\alpha\beta\gamma} \bar{c}_\alpha\, [cu]_{\beta,s=0,1}\, [ud]_{\gamma,s=0,1}, \tag{21}$$

$$\mathbb{P}_d = \epsilon^{\alpha\beta\gamma} \bar{c}_\alpha\, [cd]_{\beta,s=0,1}\, [uu]_{\gamma,s=1}, \tag{22}$$

the difference being that the $\mathbb{P}_d$ involves a $[uu]$ diquark, and the Pauli exclusion principle implies that this diquark has to be in an $SU(3)_F$-symmetric representation. This leads to two distinct $SU(3)_F$ series of pentaquarks

$$\begin{aligned} \mathbb{P}_A &= \epsilon^{\alpha\beta\gamma}\, \{\bar{c}_\alpha\, [cq]_{\beta,s=0,1}\, [q'q'']_{\gamma,s=0}, L\} = \mathbf{3} \otimes \bar{\mathbf{3}} = \mathbf{1} \oplus \mathbf{8}, \\ \mathbb{P}_S &= \epsilon^{\alpha\beta\gamma}\, \{\bar{c}_\alpha\, [cq]_{\beta,s=0,1}\, [q'q'']_{\gamma,s=1}, L\} = \mathbf{3} \otimes \mathbf{6} = \mathbf{8} \oplus \mathbf{10}. \end{aligned} \tag{23}$$

For S waves, the first and the second series have the angular momenta

$$\mathbb{P}_A(L=0): \quad J = 1/2(2),\ 3/2(1), \tag{24}$$

$$\mathbb{P}_S(L=0): \quad J = 1/2(3),\ 3/2(3),\ 5/2(1), \tag{25}$$

where the multiplicities are given in parentheses. One assigns $\mathbb{P}(3/2^-)$ to the $\mathbb{P}_A$ and $\mathbb{P}(5/2^+)$ to the $\mathbb{P}_S$ series of pentaquarks [87].

The decay amplitudes of interest can be generically written as

$$\mathcal{A} = \left\langle \mathcal{PM} \left| H_{\rm eff}^W \right| \mathcal{B} \right\rangle, \tag{26}$$

where, $H_{\rm eff}^W$ is the effective weak Hamiltonian inducing the Cabibbo-allowed $\Delta I = 0, \Delta S = -1$ transition $b \to c\bar{c}s$, and the Cabibbo-suppressed $\Delta S = 0$ transition $b \to c\bar{c}d$. The $SU(3)_F$ based analysis of the decays $\Lambda_b \to \mathbb{P}^+ K^- \to (J/\psi\, p)K^-$ goes as follows. With respect to $SU(3)_F$, $\Lambda_b(bud) \sim \bar{3}$ and it is an isosinglet $I = 0$. Thus, the weak non-leptonic Hamiltonian for $b \to c\bar{c}q$ $(q = s, d)$ decays is:

$$H_{\rm eff}^W = \frac{4G_F}{\sqrt{2}} \left[V_{cb}V_{cq}^*(c_1 O_1^{(q)} + c_2 O_2^{(q)}) \right]. \tag{27}$$

Here, G_F is the Fermi coupling constant, V_{ij} are the CKM matrix elements, and c_i are the Wilson coefficients of the operators $O_1^{(q)}$ $(q = d,\ s)$, defined as

$$O_1^{(q)} = (\bar{q}_\alpha c_\beta)_{V-A}(\bar{c}_\alpha b_\beta)_{V-A}; \quad O_2^{(q)} = (\bar{q}_\alpha c_\alpha)_{V-A}(\bar{c}_\beta b_\beta)_{V-A}, \tag{28}$$

where α and β are $SU(3)$ color indices, and $V - A = 1 - \gamma_5$ reflects that the charged currents are left-handed, and the penguin amplitudes are ignored. With M a nonet of $SU(3)$ light mesons (π, K, η, η'), the weak transitions $\langle \mathbb{P}, M|H_{\rm W}|\Lambda_b\rangle$ requires $\mathbb{P} + M$ to be in $8 \oplus 1$ representation. Recalling the $SU(3)$ group multiplication rule

$$\begin{aligned} 8 \otimes 8 &= 1 \oplus 8 \oplus 8 \oplus 10 \oplus \bar{10} \oplus 27, \\ 8 \otimes 10 &= 8 \oplus 10 \oplus 27 \oplus 35, \end{aligned} \tag{29}$$

the decay $\langle \mathbb{P}, M|H_{\rm W}|\Lambda_b\rangle$ can be realized with $\mathbb{P}$ in either an octet $\mathtt{8}$ or a decuplet $\mathtt{10}$. The discovery channel $\Lambda_b \to \mathbb{P}^+ K^- \to J/\psi p K^-$ corresponds to $\mathbb{P}$ in an octet $\mathtt{8}$.

5.2 An effective Hamiltonian for the hidden charm pentaquarks

Keeping the basic building blocks of the pentaquarks to be quarks and diquarks, we follow here the template in which the two P_c states are assumed to be made from four quarks, consisting of two highly correlated diquark pairs, and an antiquark. For the present discussion, it is an anti-charm quark $\bar{c}$ which is correlated with the two diquarks $[cq]$ and $[q'q'']$, where q, q', q'' can be u or d. The tetraquark formed by the diquark-diquark $([cq]_{\bar{\mathtt{3}}}[q'q'']_{\bar{\mathtt{3}}})$ is a color-triplet object, following from $\bar{\mathtt{3}} \times \bar{\mathtt{3}} = \bar{\mathtt{6}} + \mathtt{3}$, with orbital and spin quantum numbers, denoted by $L_{\mathcal{QQ}}$ and $S_{\mathcal{QQ}}$, which combines with the color-anti-triplet $\bar{\mathtt{3}}$ of the $\bar{c}$ to form an overall color-singlet pentaquark, with the corresponding quantum numbers $L_{\mathcal{P}}$ and $S_{\mathcal{P}}$. This is shown schematically in Fig. 16.

An effective Hamiltonian based on this picture is constructed [94], extending the underlying tetraquark Hamiltonian developed for the X, Y, Z states [32]. It involves the constituent diquarks masses, $m_{[cq]}$, $m_{[q'q'']}$, the spin-spin interactions between the quarks in each diquark shell, and the spin-orbit and orbital angular momentum of the tetraquarks. To this are added the charm quark mass m_c, the spin-orbit and the orbital terms of the pentaquarks.

$$H = H_{[\mathcal{QQ}']} + H_{\bar{c}[\mathcal{QQ}']} + H_{S_{\mathcal{P}}L_{\mathcal{P}}} + H_{L_{\mathcal{P}}L_{\mathcal{P}}}, \tag{30}$$

where the diquarks $[cq]$ and $[q'q'']$ are denoted by $\mathcal{Q}$ and $\mathcal{Q}'$ having masses $m_{\mathcal{Q}}$ and $m_{\mathcal{Q}'}$, respectively. $L_{\mathcal{P}}$ and $S_{\mathcal{P}}$ are the orbital angular momentum and the spin of the pentaquark state, and the quantities $A_{\mathcal{P}}$ and $B_{\mathcal{P}}$ parametrize the strength of their spin-orbit and orbital angular momentum couplings, respectively. The individual terms in the Hamiltonian (30) are given in [94].

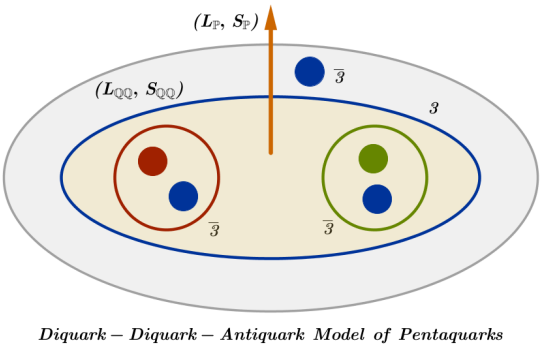

Figure 16: $SU(3)$-color quantum numbers of the diquarks, tetraquark and antiquark are indicated, together with the orbital and spin quantum numbers of the tetraquark and pentaquark [94]

.

The mass formula for the pentaquark state with the ground state tetraquark ($L_{\mathcal{QQ}'} = 0$) can be written as

$$M = M_0 + \frac{B_{\mathcal{P}}}{2} L_{\mathcal{P}}(L_{\mathcal{P}}+1) + 2A_{\mathcal{P}} \frac{J_{\mathcal{P}}(J_{\mathcal{P}}+1) - L_{\mathcal{P}}(L_{\mathcal{P}}+1) - S_{\mathcal{P}}(S_{\mathcal{P}}+1)}{2} + \Delta M \qquad (31)$$

where $M_0 = m_{\mathcal{Q}} + m_{\mathcal{Q}'} + m_c$ and ΔM is the mass term that arises from different spin-spin interactions. With the tetraquark in $L_{\mathcal{QQ}'} = 1$, one has to add the two terms given above with their coefficients $A_{\mathcal{QQ}'}$ and $B_{\mathcal{QQ}'}$. In this work, we restrict ourselves to the S-wave tetraquarks.

For $L_{\mathcal{P}} = 0$, the pentaquark states are classified in terms of the diquarks spins, $S_{\mathcal{Q}}$ and $S_{\mathcal{Q}'}$; the spin of anti-charm quark is $S_{\bar{c}} = 1/2$. There are four S-wave pentaquark states for $J^P = \frac{3}{2}^-$ and a single state with $J^P = \frac{5}{2}^-$. For $J^P = \frac{3}{2}^-$, we have the following states[3]:

$$\begin{aligned}
|0_{\mathcal{Q}}, 1_{\mathcal{Q}'}, \frac{1}{2}_{\bar{c}}; \frac{3}{2}\rangle_1 &= \frac{1}{\sqrt{2}}[(\uparrow)_c(\downarrow)_q - (\downarrow)_c(\uparrow)_q](\uparrow)_{q'}(\uparrow)_{q''}(\uparrow)_{\bar{c}} \\
|1_{\mathcal{Q}}, 0_{\mathcal{Q}'}, \frac{1}{2}_{\bar{c}}; \frac{3}{2}\rangle_2 &= \frac{1}{\sqrt{2}}[(\uparrow)_{q'}(\downarrow)_{q''} - (\downarrow)_{q'}(\uparrow)_{q''}](\uparrow)_c(\uparrow)_q(\uparrow)_{\bar{c}} \\
|1_{\mathcal{Q}}, 1_{\mathcal{Q}'}, \frac{1}{2}_{\bar{c}}; \frac{3}{2}\rangle_3 &= \frac{1}{\sqrt{6}}(\uparrow)_c(\uparrow)_q\{2(\uparrow)_{q'}(\uparrow)_{q''}(\downarrow)_{\bar{c}} - [(\uparrow)_{q'}(\downarrow)_{q''} + (\downarrow)_{q'}(\uparrow)_{q''}](\uparrow)_{\bar{c}}\} \\
|1_{\mathcal{Q}}, 1_{\mathcal{Q}'}, \frac{1}{2}_{\bar{c}}; \frac{3}{2}\rangle_4 &= \sqrt{\frac{3}{10}}[(\uparrow)_c(\downarrow)_q + (\downarrow)_c(\uparrow)_q](\uparrow)_{q'}(\uparrow)_{q''}(\uparrow)_{\bar{c}} - \sqrt{\frac{2}{15}}(\uparrow)_c(\uparrow)_q\{(\uparrow)_{q'}(\uparrow)_{q''}(\downarrow)_{\bar{c}} \\
&\quad + [(\uparrow)_{q'}(\downarrow)_{q''} + (\downarrow)_{q'}(\uparrow)_{q''}](\uparrow)_{\bar{c}}\}, \qquad (32)
\end{aligned}$$

and the spin representation corresponding to $J^P = \frac{5}{2}^-$ state is:

$$|1_{\mathcal{Q}}, 1_{\mathcal{Q}'}, \frac{1}{2}_{\bar{c}}; \frac{5}{2}\rangle = (\uparrow)_c(\uparrow)_q(\uparrow)_{q'}(\uparrow)_{q''}(\uparrow)_{\bar{c}}\,. \qquad (33)$$

[3]For a similar classification in the diquark-triquark picture, see[96].

Table 6: S (P)- wave pentaquark states $\mathcal{P}_{X_i}$ $(\mathcal{P}_{Y_i})$ and their spin- and orbital angular momentum quantum numbers. The subscripts $\mathcal{Q}$ and $\mathcal{Q}'$ represent the heavy $[cq]$ and light $[q'q'']$ diquarks, respectively. In the expressions for the masses of the $\mathcal{P}_{Y_i}$ states, the terms $M_{\mathcal{P}_{X_i}} = M_0 + \Delta M_i$ with $i = 1, ..., 5$.

Label	$\lvert S_\mathcal{Q}, S_{\mathcal{Q}'}; L_\mathcal{P}, J^P\rangle_i$	Mass	Label	$\lvert S_\mathcal{Q}, S_{\mathcal{Q}'}; L_\mathcal{P}, J^P\rangle_i$	Mass
$\mathcal{P}_{X_1}$	$\lvert 0_\mathcal{Q}, 1_{\mathcal{Q}'}, 0; \frac{3}{2}^-\rangle_1$	$M_0 + \Delta M_1$	$\mathcal{P}_{Y_1}$	$\lvert 0_\mathcal{Q}, 1_{\mathcal{Q}'}, 1; \frac{5}{2}^+\rangle_1$	$M_{\mathcal{P}_{X_1}} + 3A_\mathcal{P} + B_\mathcal{P}$
$\mathcal{P}_{X_2}$	$\lvert 1_\mathcal{Q}, 0_{\mathcal{Q}'}, 0; \frac{3}{2}^-\rangle_2$	$M_0 + \Delta M_2$	$\mathcal{P}_{Y_2}$	$\lvert 1_\mathcal{Q}, 0_{\mathcal{Q}'}, 1; \frac{5}{2}^+\rangle_2$	$M_{\mathcal{P}_{X_2}} + 3A_\mathcal{P} + B_\mathcal{P}$
$\mathcal{P}_{X_3}$	$\lvert 1_\mathcal{Q}, 1_{\mathcal{Q}'}, 0; \frac{3}{2}^-\rangle_3$	$M_0 + \Delta M_3$	$\mathcal{P}_{Y_3}$	$\lvert 1_\mathcal{Q}, 1_{\mathcal{Q}'}, 1; \frac{5}{2}^+\rangle_3$	$M_{\mathcal{P}_{X_3}} + 3A_\mathcal{P} + B_\mathcal{P}$
$\mathcal{P}_{X_4}$	$\lvert 1_\mathcal{Q}, 1_{\mathcal{Q}'}, 0; \frac{3}{2}^-\rangle_4$	$M_0 + \Delta M_4$	$\mathcal{P}_{Y_4}$	$\lvert 1_\mathcal{Q}, 1_{\mathcal{Q}'}, 1; \frac{5}{2}^+\rangle_4$	$M_{\mathcal{P}_{X_4}} + 3A_\mathcal{P} + B_\mathcal{P}$
$\mathcal{P}_{X_5}$	$\lvert 1_\mathcal{Q}, 1_{\mathcal{Q}'}, 0; \frac{5}{2}^-\rangle_5$	$M_0 + \Delta M_5$	$\mathcal{P}_{Y_5}$	$\lvert 1_\mathcal{Q}, 1_{\mathcal{Q}'}, \frac{1}{2}_{\bar{c}}, 1; \frac{5}{2}^+\rangle_5$	$M_{\mathcal{P}_{X_5}} - 2A_\mathcal{P} + B_\mathcal{P}$

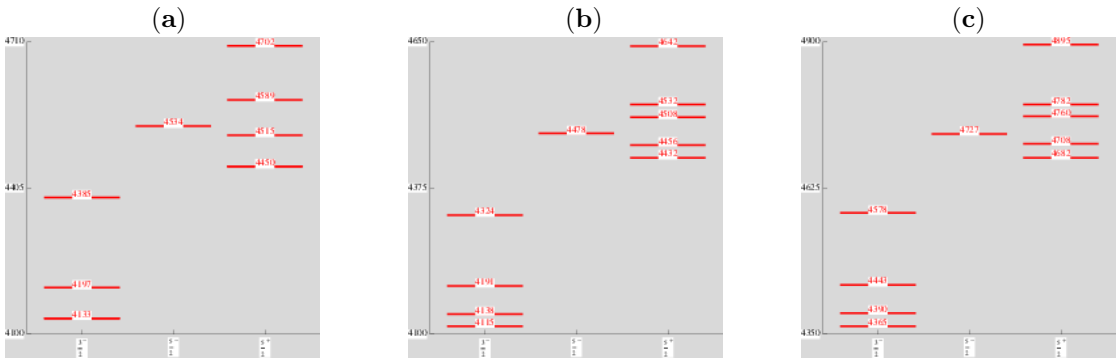

Figure 17: Mass Spectrum (in MeV) of the lowest S- and P-wave pentaquark states in the diquark-diquark-antiquark picture for the charmonium sector for the flavor content (a) $\bar{c}[cq][qq]$, (b) $\bar{c}[cq][sq]$, and (c) $\bar{c}[cs][qq]$. (from [94])

The masses for the four S-wave pentaquark states with $J^P = \frac{3}{2}^-$ and a single state with $J^P = \frac{5}{2}^-$ are given in Table 6, where we label the states as $\mathcal{P}_{X_i}$. The corresponding five P-wave pentaquark states with $L_\mathcal{P} = 1$ and $J^P = \frac{5}{2}^+$ are labeled as $\mathcal{P}_{Y_i}$ in Table 6. ΔM_i are defined in [94], where also the various input parameters are given. The resulting mass spectrum with the quark flavor content $\bar{c}[cq][qq]$, $\bar{c}[cq][sq]$, and $\bar{c}[cs][qq]$, characterized by $c_i (i = 1, 2, 3)$, respectively, is shown in Fig. 17. The above figure shows that the spectrum of pentaquark states in the compact diquark model is very rich. For comparison with the current LHC data, only the left frame in Fig. 17 is relevant. Apart from the other predicted states, there is a state, $\mathcal{P}_{X_4}$, which is predicted to have a mass 4385 MeV, having the quantum numbers $|1_\mathcal{Q}, 1_{\mathcal{Q}'}, 0; \frac{3}{2}^-\rangle$. This agrees with the mass of the observed state $P_c^+(4380)$. Likewise, the state $P_c^+(4550)$, having $J^P = \frac{5}{2}^+$ can be identified with the state $\mathcal{P}_{Y_2}$ in the firs t row of Table 6, having the quantum numbers $|1_\mathcal{Q}, 0_{\mathcal{Q}'}, 1; \frac{5}{2}^+\rangle$. We recall that these two states have the same internal

quantum numbers as assumed by Maiani *et al.* [87]:

$$P_c(4380)^+ = \mathbb{P}^+(3/2^-) = \{\bar{c}\,[cq]_{s=1}[q'q'']_{s=1}, L=0\}\,,$$
$$P_c(4450)^+ = \mathbb{P}^+(5/2^+) = \{\bar{c}\,[cq]_{s=1}[q'q'']_{s=0}, L=1\}\,. \quad (34)$$

5.3 b-baryonn decays to pentaquarks and heavy quark symmetry

The pentaquark states reported by the LHCb are produced in Λ_b^0 decays, $\Lambda_b^0 \to \mathcal{P}^+\, K^-$, where $\mathcal{P}$ denotes a generic pentaquark state. QCD has a symmetry in the heavy quark limit, i.e., for $m_b \gg \Lambda_{\rm QCD}$, b-quark becomes a static quark and the light diquark spin becomes a good quantum number, constraining the states which can otherwise be produced. The b-baryon decays to pentaquarks having a $c\bar{c}$ component are also presumably subject to the selection rules following from the heavy quark symmetry. Thus, the state $\mathcal{P}_{X_4}$ (identified with $P_c(4380)^+$ in [87]) is unlikely to be produced in Λ_b decays, as it has the "wrong" light-diquark spin number. On the other hand, there is a lower mass state $\mathcal{P}_{X_2}$ present in the spectrum, having the correct flavor and spin quantum numbers $|1_Q, 0_{Q'}, 0; \frac{3}{2}^-\rangle$, with a mass of about 4130 MeV, which we expect to be produced in Λ_b decays. One could argue that the mass estimates following from the assumed effective Hamiltonian are in error by a larger amount than quoted in [94]. However, as already stated, the mass difference between the $J^P = \frac{5}{2}^+$ and $J^P = \frac{3}{2}^-$ pentaquarks, having the right quantum numbers $|1_{\mathcal{Q}}, 0_{\mathcal{Q}'}, 1; \frac{5}{2}^+\rangle$ and $|1_{\mathcal{Q}}, 0_{\mathcal{Q}'}, 0; \frac{3}{2}^-\rangle$ is expected to be around 340 MeV, yielding a mass for the lower-mass $J^P = \frac{3}{2}^-$ pentaquark state of about 4110 MeV. The two estimates are compatible with each other, and we advocate to search for this state in the LHCb data. Among the ten states listed in Table 6, only the ones called $\mathcal{P}_{X_2}$ and $\mathcal{P}_{Y_2}$ are allowed as the Λ_b decay products.

5.4 Weak decays with $\mathbb{P}$ in Decuplet representation

Decays involving the decuplet `10` pentaquarks may also occur, if the light diquark pair having spin-0 $[ud]_{s=0}$ in Λ_b gets broken to produce a spin-1 light diquark $[ud]_{s=1}$. In this case, one would also observe the decays of Λ_b, such as

$$\Lambda_b \to \pi \mathbb{P}_{10}^{(S=-1)} \to \pi(J/\psi\Sigma(1385)),$$
$$\Lambda_b \to K^+ \mathbb{P}_{10}^{(S=-2)} \to K^+(J/\psi\Xi^-(1530)).$$

These decays are, however, disfavored by the heavy-quark-spin-conservation selection rules. The extent to which this rule is compatible with the existing data on B-meson and Λ_b decays can be seen in the PDG entries. Whether the decays of the pentaquarks are also subject to the same selection rules is yet to be checked, but on symmetry grounds, we do expect it to hold. Hence, the observation (or not) of these decays will be quite instructive.

Apart from $\Lambda_b(bud)$, several other b-baryons, such as $\Xi_b^0(usb)$, $\Xi_b^-(dsb)$ and $\Omega_b^-(ssb)$ undergo weak decays. These b-baryons are characterized by the spin of the light diquark, as shown below, making their isospin (I) and strangeness (S) quantum numbers explicit as well as their light diquark $j^{\rm P}$ quantum numbers. The c-baryons are likewise characterized similarly.
Examples of bottom-strange b-baryon in various charge combinations, respecting $\Delta I = 0$, $\Delta S = -1$ are:

$$\Xi_b^0(5794) \to K(J/\psi\Sigma(1385)),$$

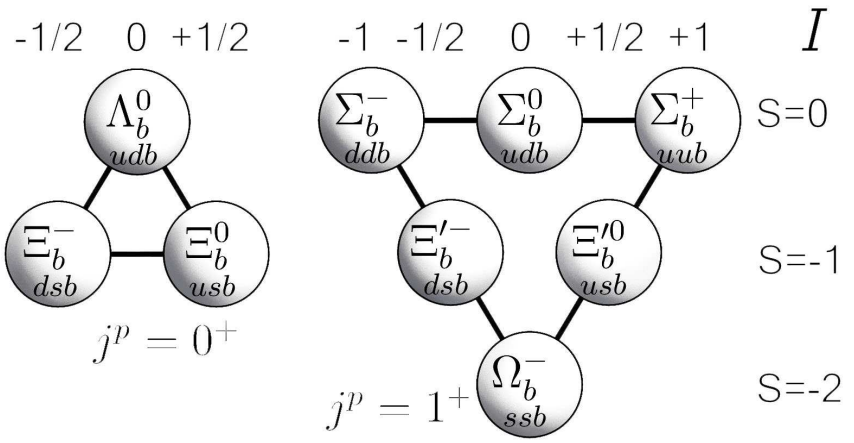

Figure 18: b-baryons with the light diquark spins $j^p = 0^+$ (left) and $j^p = 1^+$ (right).

which corresponds to the formation of the pentaquarks with the spin configuration $\mathbb{P}_{10}(\bar{c}\,[cq]_{s=0,1}\,[q's]_{s=0,1})$ with $(q, q' = u, d)$.
Above considerations have been extended involving the entire $SU(3)_F$ multiplets entering the generic decay amplitude $\langle \mathcal{P}\mathcal{M}|H_{\rm eff}|\mathcal{B}\rangle$, where $\mathcal{B}$ is the $SU(3)_F$ antitriplet b-baryon, shown in the left frame of Fig. 18, $\mathcal{M}$ is the 3×3 pseudoscalar meson matrix

$$\mathcal{M}_i^j = \begin{pmatrix} \frac{\pi^0}{\sqrt{2}} + \frac{\eta_8}{\sqrt{6}} & \pi^+ & K^+ \\ \pi^- & -\frac{\pi^0}{\sqrt{2}} + \frac{\eta_8}{\sqrt{6}} & K^0 \\ K^- & \bar{K}^0 & -\frac{2\eta_8}{\sqrt{6}} \end{pmatrix},$$

and $\mathcal{P}$ is a pentaquark state belonging to an octet with definite J^P, denoted as a 3×3 matrix J^P, $\mathcal{P}_j^i(J^{\rm P})$,

$$\mathcal{P}_i^j\left(J^P\right) = \begin{pmatrix} \frac{P_{\Sigma^0}}{\sqrt{2}} + \frac{P_\Lambda}{\sqrt{6}} & P_{\Sigma^+} & P_p \\ P_{\Sigma^-} & -\frac{P_{\Sigma^0}}{\sqrt{2}} + \frac{P_\Lambda}{\sqrt{6}} & P_n \\ P_{\Xi^-} & P_{\Xi^0} & -\frac{P_\Lambda}{\sqrt{6}} \end{pmatrix},$$

or a decuplet $\mathcal{P}_{ijk}$ (symmetric in the indices), with $\mathcal{P}_{111} = \Delta_{10}^{++}, ..., \mathcal{P}_{333} = \Omega_{10}^-$. (see Guan-Nan Li *et al.* [88] for a detailed list of the component fields and $SU(3)_F$-based relations among decay widths). The two observed pentaquarks are denoted as $P_p(3/2^-)$ and $P_p(5/2^+)$.

Estimates of the $SU(3)$ amplitudes require a dynamical model, which will be lot more complex to develop than the factorization-based models for the two-body B-meson decays, but, as argued in the literature, SU(3) symmetry can be used to relate different decay modes. Using heavy quark symmetry, which reduces the number of Feynman diagrams to be calculated, they are worked out in [94]. Thus, the decay $\Lambda_b^0 \to J/\psi p K^-$ and $\Lambda_b^0 \to J/\psi p \pi^-$ have just one dominant Feynman diagram each, the one in which the $[ud]$ diquark in Λ_b^0 retains its spin. The ratio of the branching fraction $\mathcal{B}(\Lambda_b^0 \to J/\psi p \pi^)/\mathcal{B}(\Lambda_b^0 \to J/\psi p K^-) = 0.0824 \pm 0.0024 \pm 0.0042$ [98] is consistent with the expectations from Cabibbo suppression. This ratio

should also hold for the resonating part of the amplitudes, namely if one replaces the $J/\psi p$ by $P_c(4450)^+$, and like wise for the $J^P = 3/2^-$ P_c^+ state. This is hinted by the current LHCb measurements [99].

Examples of the weak decays in which the initial b-baryon has a spin-1 light diquark, i.e. $j^{\rm P} = 1^+$, which is retained in the transition, are provided by the Ω_b decays. The $s\bar{s}$ pair in Ω_b is in the symmetric $\mathsf{6}$ representation of $SU(3)_F$ with spin 1 and is expected to produce decuplet pentaquarks in association with a ϕ or a kaon [87]

$$\Omega_b(6049) \to \phi(J/\psi\,\Omega^-(1672)), K(J/\psi\,\Xi(1387)).$$

These correspond, respectively, to the formation of the following pentaquarks ($q = u,\, d$)

$$\mathbb{P}_{10}^-(\bar{c}\,[cs]_{s=0,1}\,[ss]_{s=1}), \mathbb{P}_{10}(\bar{c}\,[cq]_{s=0,1}\,[ss]_{s=1}).$$

These transitions are expected on firmer theoretical footings, as the initial $[ss]$ diquark in Ω_b is left unbroken. Again, a lot more transitions can be found relaxing this condition, which would involve a $j^{\rm P} = 1^+ \to 0^+$ light diquark, but they are anticipated to be suppressed.

6 Summary

In summary, with the discoveries of the X, Y, Z and P_c states a new era of hadron spectroscopy is upon us. In addition to the well-known $q\bar{q}$ mesons and qqq baryons, there is increasing evidence that the hadronic world is multi-layered, in the form of tetraquark mesons, pentaquark baryons, and likely also the hexaquarks (or H dibaryons) [100]. However, the underlying dynamics is far from being understood, and the real issue is how the various constituents of an exotic multiquark state rearrange themselves. The two competing pictures are hadron molecules and compact diquak models, with $Q\bar{Q}g$ hybrids and glueballs also anticipated. Thresholds near the resonances do play a role in the phenomenology, and in some cases kinematic-induced cusp effects may also be a viable template. It is plausible, perhaps rather likely, that no single mechanism fits all the observable states, and the exotic hadrons may find their abode in competing theoretical frameworks. The case of diquark models in this context was reviewed here in more detail. Existence proof on the lattice of diquark correlations in some of the tetra- and pentaquark states discussed here would be a breakthrough and keenly awaited. In the meanwhile, phenomenological models built within constrained theoretical frameworks are unavoidable. They and experiments will guide us how to navigate through this uncharted territory.

7 Acknowledgments

I would like to thank the local organizers of the Helmholtz school "Quantum Field Theory at the Limits: From Strong Fields to Heavy Quarks", and JINR for their warm hospitality. Helpful discussions with Sören Lange, Luciano Maiani, Antonello Polosa, and Sheldon Stone are thankfully acknowledged. Thanks are also due to Sheldon Stone for craefully reading the manuscript.

References

[1] S.-K. Choi *et al.* (Belle Collaboration), Phys. Rev. Lett. **91**, 262001 (2003).

[2] R. Aaij *et al.* [LHCb Collaboration], Phys. Rev. Lett. **115** (2015) 072001 [arXiv:1507.03414 [hep-ex]].

[3] A. Esposito, A. Pilloni and A. D. Polosa, arXiv:1611.07920 [hep-ph].

[4] E. S. Swanson, Int. J. Mod. Phys. E **25**, no. 07, 1642010 (2016) doi:10.1142/S0218301316420106 [arXiv:1504.07952 [hep-ph]].

[5] E. S. Swanson, Phys. Rev. D **91** (2015) no.3, 034009 [arXiv:1409.3291 [hep-ph]].

[6] E. P. Wigner, Phys. Rev. **73**, 1002 (1948).

[7] N. A. Tornqvist, Z. Phys. C **68**, 647 (1995) [hep-ph/9504372].

[8] D. V. Bugg, J. Phys. G **35**, 075005 (2008) [arXiv:0802.0934 [hep-ph]].

[9] S. Dubynskiy and M. B. Voloshin, Phys. Lett. B **666**, 344 (2008) [arXiv:0803.2224 [hep-ph]].

[10] F. E. Close and P. R. Page, Nucl. Phys. B **443**, 233 (1995) [hep-ph/9411301].

[11] J. J. Dudek, Phys. Rev. D **84**, 074023 (2011) [arXiv:1106.5515 [hep-ph]].

[12] S. M. Ryan, EPJ Web Conf. **130**, 01002 (2016).

[13] F. E. Close and P. R. Page, Phys. Lett. B **628**, 215 (2005) [hep-ph/0507199].

[14] E. Kou and O. Pene, Phys. Lett. B **631**, 164 (2005) [hep-ph/0507119].

[15] S. L. Zhu, Phys. Lett. B **625**, 212 (2005) [hep-ph/0507025].

[16] C. A. Meyer and E. S. Swanson, Prog. Part. Nucl. Phys. **82**, 21 (2015) [arXiv:1502.07276 [hep-ph]].

[17] M. R. Pennington, EPJ Web Conf. **113** (2016) 01014 [arXiv:1509.02555 [nucl-th]].

[18] M. Berwein, N. Brambilla, J. Tarrs Castell and A. Vairo, Phys. Rev. D **92** (2015) no.11, 114019 [arXiv:1510.04299 [hep-ph]].

[19] H. Al Ghoul *et al.* [GlueX Collaboration], AIP Conf. Proc. **1735**, 020001 (2016) [arXiv:1512.03699 [nucl-ex]].

[20] M. F. M. Lutz *et al.* [PANDA Collaboration], arXiv:0903.3905 [hep-ex].

[21] N. A. Tornqvist, Z. Phys. C **61**, 525 (1994) [hep-ph/9310247]; E. Braaten and M. Kusunoki, Phys. Rev. D **69**, 074005 (2004) [hep-ph/0311147]; F. E. Close and P. R. Page, Phys. Lett. B **578**, 119 (2004) [hep-ph/0309253]; E. S. Swanson, Phys. Rept. **429**, 243 (2006) [hep-ph/0601110]; M. Cleven, F. K. Guo, C. Hanhart and U. G. Meissner, Eur. Phys. J. A **47**, 120 (2011) [arXiv:1107.0254 [hep-ph]].

[22] C. Bignamini, B. Grinstein, F. Piccinini, A. D. Polosa and C. Sabelli, Phys. Rev. Lett. **103**, 162001 (2009) [arXiv:0906.0882 [hep-ph]].

[23] P. Artoisenet and E. Braaten, Phys. Rev. D **81**, 114018 (2010) [arXiv:0911.2016 [hep-ph]].

[24] T. Gutsche, M. Kesenheimer and V. E. Lyubovitskij, Phys. Rev. D **90**, no. 9, 094013 (2014) [arXiv:1410.0259 [hep-ph]].

[25] M. Cleven, arXiv:1405.4195 [hep-ph].

[26] F.-K. Guo, C. Hanhart, Y. S. Kalashnikova, P. Matuschek, R. V. Mizuk, A. V. Nefediev, Q. Wang and J.-L. Wynen, Phys. Rev. D **93**, no. 7, 074031 (2016) [arXiv:1602.00940 [hep-ph]].

[27] P. Artoisenet, E. Braaten and D. Kang, Phys. Rev. D **82**, 014013 (2010) [arXiv:1005.2167 [hep-ph]].

[28] C. Hanhart, Y. S. Kalashnikova and A. V. Nefediev, Eur. Phys. J. A **47**, 101 (2011) [arXiv:1106.1185 [hep-ph]].

[29] C. Meng, J. J. Sanz-Cillero, M. Shi, D. L. Yao and H. Q. Zheng, Phys. Rev. D **92**, no. 3, 034020 (2015) [arXiv:1411.3106 [hep-ph]].

[30] T. Barnes, F. E. Close and E. S. Swanson, Phys. Rev. D **91**, no. 1, 014004 (2015) [arXiv:1409.6651 [hep-ph]].

[31] L. Maiani, F. Piccinini, A. D. Polosa and V. Riquer, Phys. Rev. Lett. **93** (2004) 212002 [hep-ph/0407017].

[32] L. Maiani, F. Piccinini, A. D. Polosa and V. Riquer, Phys. Rev. D **71**, 014028 (2005) [hep-ph/0412098].

[33] S. J. Brodsky, D. S. Hwang and R. F. Lebed, Phys. Rev. Lett. **113**, no. 11, 112001 (2014) [arXiv:1406.7281 [hep-ph]].

[34] S. Weinberg, Phys. Rev. Lett. **110**, 261601 (2013) [arXiv:1303.0342 [hep-ph]].

[35] M. Knecht and S. Peris, Phys. Rev. D **88**, 036016 (2013) [arXiv:1307.1273 [hep-ph]].

[36] G. Rossi and G. Veneziano, JHEP **1606**, 041 (2016) [arXiv:1603.05830 [hep-th]].

[37] M. Padmanath, C. B. Lang and S. Prelovsek, Phys. Rev. D **92**, no. 3, 034501 (2015) [arXiv:1503.03257 [hep-lat]].

[38] A. Hosaka, T. Iijima, K. Miyabayashi, Y. Sakai and S. Yasui, PTEP **2016**, no. 6, 062C01 (2016) [arXiv:1603.09229 [hep-ph]].

[39] C. DeTar, PoS LeptonPhoton **2015**, 023 (2016) [arXiv:1511.06884 [hep-lat]].

[40] Y. Chen *et al.*, Phys. Rev. D **89**, no. 9, 094506 (2014) [arXiv:1403.1318 [hep-lat]].

[41] Y. Ikeda *et al.* [HAL QCD Collaboration], Phys. Rev. Lett. **117**, no. 24, 242001 (2016) [arXiv:1602.03465 [hep-lat]].

[42] L. Maiani, F. Piccinini, A. D. Polosa and V. Riquer, Phys. Rev. D **89**, 114010 (2014) [arXiv:1405.1551 [hep-ph]].

[43] A. Ali, C. Hambrock, I. Ahmed and M. J. Aslam, Phys. Lett. B **684**, 28 (2010) [arXiv:0911.2787 [hep-ph]].

[44] A. Ali, C. Hambrock and M. J. Aslam, Phys. Rev. Lett. **104**, 162001 (2010) Erratum: [Phys. Rev. Lett. **107**, 049903 (2011)] [arXiv:0912.5016 [hep-ph]].

[45] A. Ali, C. Hambrock and S. Mishima, Phys. Rev. Lett. **106**, 092002 (2011) [arXiv:1011.4856 [hep-ph]].

[46] R. A. Briceno *et al.*, Chin. Phys. C **40** (2016) no.4, 042001 [arXiv:1511.06779 [hep-ph]].

[47] H. X. Chen, W. Chen, X. Liu and S. L. Zhu, Phys. Rept. **639**, 1 (2016) [arXiv:1601.02092 [hep-ph]].

[48] R. F. Lebed, R. E. Mitchell and E. S. Swanson, arXiv:1610.04528 [hep-ph].

[49] R. L. Jaffe, Phys. Rept. **409**, 1 (2005) [hep-ph/0409065].

[50] C. Alexandrou, P. de Forcrand and B. Lucini, Phys. Rev. Lett. **97**, 222002 (2006) [hep-lat/0609004].

[51] A. V. Manohar and M. B. Wise, Camb. Monogr. Part. Phys. Nucl. Phys. Cosmol. **10**, 1 (2000).

[52] M. Karliner, J. L. Rosner and S. Nussinov, arXiv:1611.00348 [hep-ph]; Z. G. Wang, arXiv:1701.04285 [hep-ph]; Y. Bai, S. Lu and J. Osborne, arXiv:1612.00012 [hep-ph].

[53] A. Ali, L. Maiani, A. D. Polosa and V. Riquer, Phys. Rev. D **91**, no. 1, 017502 (2015) [arXiv:1412.2049 [hep-ph]].

[54] D. Ebert, R. N. Faustov and V. O. Galkin, Phys. Lett. B **634**, 214 (2006) [hep-ph/0512230].

[55] M. Nielsen, F. S. Navarra and S. H. Lee, Phys. Rept. **497**, 41 (2010) [arXiv:0911.1958 [hep-ph]].

[56] R. Albuquerque, S. Narison, F. Fanomezana, A. Rabemananjara, D. Rabetiarivony and G. Randriamanatrika, Int. J. Mod. Phys. A **31**, no. 36, 1650196 (2016) [arXiv:1609.03351 [hep-ph]].

[57] A. Ali, L. Maiani, A. D. Polosa and V. Riquer, Phys. Rev. D **94**, no. 3, 034036 (2016) [arXiv:1604.01731 [hep-ph]].

[58] V. M. Abazov *et al.* [D0 Collaboration], Phys. Rev. Lett. **117** (2016) no.2, 022003 [arXiv:1602.07588 [hep-ex]].

[59] The LHCb Collaboration [LHCb Collaboration], LHCb-CONF-2016-004, CERN-LHCb-CONF-2016-004.

[60] S. S. Agaev, K. Azizi and H. Sundu, Eur. Phys. J. Plus **131**, no. 10, 351 (2016) [arXiv:1603.02708 [hep-ph]].

[61] K. F. Chen *et al.* [Belle Collaboration], Phys. Rev. Lett. **100**, 112001 (2008) [arXiv:0710.2577 [hep-ex]].

[62] N. Brambilla *et al.*, Eur. Phys. J. C **71**, 1534 (2011) [arXiv:1010.5827 [hep-ph]].

[63] D. Santel *et al.* [Belle Collaboration], Phys. Rev. D **93** (2016) no.1, 011101 [arXiv:1501.01137 [hep-ex]].

[64] G. 't Hooft, G. Isidori, L. Maiani, A. D. Polosa and V. Riquer, Phys. Lett. B **662**, 424 (2008) [arXiv:0801.2288 [hep-ph]].

[65] A. H. Fariborz, R. Jora and J. Schechter, Phys. Rev. D **77**, 094004 (2008) [arXiv:0801.2552 [hep-ph]].

[66] A. Bondar *et al.* [Belle Collaboration], Phys. Rev. Lett. **108**, 122001 (2012) [arXiv:1110.2251 [hep-ex]].

[67] R. Mizuk *et al.* [Belle Collaboration], Phys. Rev. Lett. **117**, no. 14, 142001 (2016) [arXiv:1508.06562 [hep-ex]].

[68] A. E. Bondar *et al.*, Phys. Rev. D **84**, 054010 (2011) [arXiv:1105.4473 [hep-ph]].

[69] A. Ali and W. Wang, Phys. Rev. Lett. **106**, 192001 (2011) [arXiv:1103.4587 [hep-ph]].

[70] B. Aubert *et al.* [BaBar Collaboration], Phys. Rev. D **74**, 091103 (2006) [hep-ex/0610018].

[71] M. Ablikim *et al.* [BES Collaboration], Phys. Rev. Lett. **100**, 102003 (2008) [arXiv:0712.1143 [hep-ex]].

[72] C. P. Shen *et al.* [Belle Collaboration], Phys. Rev. D **80**, 031101 (2009) [arXiv:0808.0006 [hep-ex]].

[73] N. V. Drenska, R. Faccini and A. D. Polosa, Phys. Lett. B **669**, 160 (2008) [arXiv:0807.0593 [hep-ph]].

[74] K.A. Olive *et al.* (Particle Data Group), Chinese Phys., **C 38**, 090001 (2014).

[75] See the review by G. C.Wohl in K.A. Olive *et al.* (Particle Data Group), Chinese Phys.,**C 38**, 090001 (2014).

[76] T. J. Burns, Eur. Phys. J. A **51** (2015) no.11, 152 [arXiv:1509.02460 [hep-ph]].

[77] V. Kubarovsky and M. B. Voloshin, Phys. Rev. D **92**, no. 3, 031502 (2015) [arXiv:1508.00888 [hep-ph]].

[78] F. K. Guo, U. G. Meiner, W. Wang and Z. Yang, Phys. Rev. D **92**, no. 7, 071502 (2015) [arXiv:1507.04950 [hep-ph]].

[79] X. H. Liu, Q. Wang and Q. Zhao, Phys. Lett. B **757** (2016) 231 [arXiv:1507.05359 [hep-ph]].

[80] M. Mikhasenko, arXiv:1507.06552 [hep-ph].

[81] U. G. Meiner and J. A. Oller, Phys. Lett. B **751**, 59 (2015) [arXiv:1507.07478 [hep-ph]].

[82] H. X. Chen, W. Chen, X. Liu, T. G. Steele and S. L. Zhu, Phys. Rev. Lett. **115**, no. 17, 172001 (2015) [arXiv:1507.03717 [hep-ph]].

[83] J. He, Phys. Lett. B **753**, 547 (2016) [arXiv:1507.05200 [hep-ph]].

[84] L. Roca, J. Nieves and E. Oset, Phys. Rev. D **92**, no. 9, 094003 (2015) [arXiv:1507.04249 [hep-ph]].

[85] R. Chen, X. Liu, X. Q. Li and S. L. Zhu, Phys. Rev. Lett. **115**, no. 13, 132002 (2015) [arXiv:1507.03704 [hep-ph]].

[86] C. W. Xiao and U.-G. Meiner, Phys. Rev. D **92**, no. 11, 114002 (2015) [arXiv:1508.00924 [hep-ph]].

[87] L. Maiani, A. D. Polosa and V. Riquer, Phys. Lett. B **749**, 289 (2015) [arXiv:1507.04980 [hep-ph]].

[88] G. N. Li, X. G. He and M. He, JHEP **1512**, 128 (2015) [arXiv:1507.08252 [hep-ph]].

[89] A. Mironov and A. Morozov, JETP Lett. **102**, no. 5, 271 (201 [arXiv:1507.04694 [hep-ph]].

[90] V. V. Anisovich, M. A. Matveev, J. Nyiri, A. V. Sarantsev and A. N. Semenova, arXiv:1507.07652 [hep-ph].

[91] R. Ghosh, A. Bhattacharya and B. Chakrabarti, arXiv:1508.00356 [hep-ph].

[92] Z. G. Wang, Eur. Phys. J. C **76**, no. 2, 70 (2016) [arXiv:1508.01468 [hep-ph]].

[93] Z. G. Wang and T. Huang, Eur. Phys. J. C **76**, no. 1, 43 (2016) [arXiv:1508.04189 [hep-ph]].

[94] A. Ali, I. Ahmed, M. J. Aslam and A. Rehman, Phys. Rev. D **94**, no. 5, 054001 (2016) [arXiv:1607.00987 [hep-ph]].

[95] R. F. Lebed, Phys. Lett. B **749**, 454 (2015) [arXiv:1507.05867 [hep-ph]].

[96] R. Zhu and C. F. Qiao, Phys. Lett. B **756**, 259 (2016) [arXiv:1510.08693 [hep-ph]].

[97] S. M. Flatte, Phys. Lett. **63B**, 224 (1976). doi:10.1016/0370-2693(76)90654-7

[98] R. Aaij *et al.* [LHCb Collaboration], JHEP **1407**, 103 (2014) [arXiv:1406.0755 [hep-ex]].

[99] R. Aaij *et al.* [LHCb Collaboration], Phys. Rev. Lett. **117**, no. 8, 082003 (2016) Addendum: [Phys. Rev. Lett. **117**, no. 10, 109902 (2016)] [arXiv:1606.06999 [hep-ex]].

[100] L. Maiani, A. D. Polosa and V. Riquer, Phys. Lett. B **750**, 37 (2015) [arXiv:1508.04459 [hep-ph]].